https://ntrs.nasa.gov/search.jsp?R=19800012334 2020-03-21T18:20:12+00:00Z

NOTICE

THIS DOCUMENT HAS BEEN REPRODUCED FROM MICROFICHE. ALTHOUGH IT IS RECOGNIZED THAT CERTAIN PORTIONS ARE ILLEGIBLE, IT IS BEING RELEASED IN THE INTEREST OF MAKING AVAILABLE AS MUCH INFORMATION AS POSSIBLE

JPL NO. 9950-309

(NASA-CR-162899) STUDY PROGRAM TO DEVELOP AND EVALUATE DIE AND CONTAINER MATERIALS FOR THE GROWTH OF SILICON RIBBONS Final Report (Eagle-Picher Industries, Inc., Miami, Okla.) 124 p HC A06/MF A01 CSCL 10A G3/44

N80-20818

Unclas 46755

STUDY PROGRAM TO DEVELOP AND EVALUATE DIE AND CONTAINER MATERIALS FOR THE GROWTH OF SILICON RIBBONS

Paul E. Grayson, Program Manager
Larry A. Addington, Project Engineer

Miami Research Laboratories
Eagle-Picher Industries, Inc.
Miami, Oklahoma 74354

AUTHORS: L. A. Addington, MRL
P. D. Ownby, UMR
B. B. Yu, UMR
M. W. Barsoum, UMR
H. V. Romero, UMR
B. G. Zealer, Chemetal

FINAL REPORT
DECEMBER 1979

The JPL Low-Cost Silicon Solar Array Project is funded by DOE and forms part of the DOE Photovoltaic Conversion Program to initiate a major effort toward the development of low-cost solar arrays.

Prepared Under Contract No. 954877 for

JET PROPULSION LABORATORY
CALIFORNIA INSTITUTE OF TECHNOLOGY
Pasadena, California 91103

Sponsored by the

NATIONAL AERONAUTICS AND SPACE ADMINISTRATION

Under Contract NAS7 - 100

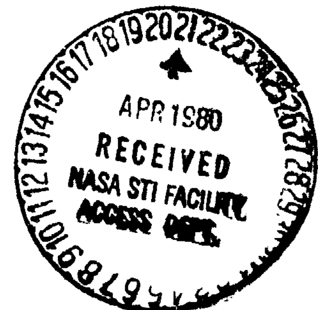

EAGLE PICHER

DOE / JPL-954877-78 / 3
Dist. Category UC-63

STUDY PROGRAM TO DEVELOP AND EVALUATE DIE AND CONTAINER MATERIALS FOR THE GROWTH OF SILICON RIBBONS

Paul E. Grayson, Program Manager
Larry A. Addington, Project Engineer

Miami Research Laboratories
Eagle-Picher Industries, Inc.
Miami, Oklahoma 74354

AUTHORS: L. A. Addington, MRL
P. D. Ownby, UMR
B. B. Yu, UMR
M. W. Barsoum, UMR
H. V. Romero, UMR
B. G. Zealer, Chemetal

FINAL REPORT
DECEMBER 1979

The JPL Low-Cost Silicon Solar Array Project is funded by DOE and forms part of the DOE Photovoltaic Conversion Program to initiate a major effort toward the development of low-cost solar arrays.

Prepared Under Contract No. 954877 for

JET PROPULSION LABORATORY
CALIFORNIA INSTITUTE OF TECHNOLOGY
Pasadena, California 91103

Sponsored by the

NATIONAL AERONAUTICS AND SPACE ADMINISTRATION

Under Contract NAS7 - 100

TECHNICAL CONTENT STATEMENT

This report contains information prepared by Eagle-Picher Industries, Inc. under JPL sub-contract. The content is not necessarily endorsed by the Jet Propulsion Laboratory, California Institute of Technology, or the National Aeronautics and Space Administration.

ACKNOWLEDGEMENT

Due to the diversity of tasks required for this program and the subcontractor involvement, the work of many people, in addition to the authors must be acknowledged. The following persons contributed valuable assistance as indicated: Mel Hagan (JPL), Technical Manager; D.D. Burt (MRL), hot pressing of containers; George Alexander (MRL), x-ray diffraction and SEM; Gene Cantwell (MRL), x-ray diffraction; Mary Holland and Billie Ginn (MRL), secretarial; Professor Thomas (PSU), x-ray diffraction; John Koen (UMR), optical microscopy; and Robert Holzl, Bob Davis, J.J. Stiglich and Brian Zealear (Chemetal), for technical and administrative input.

ABSTRACT

The Large Area Silicon Sheet Growth Task objective of lowering the cost of silicon photovoltaic material requires the development of materials which exhibit improved chemical and dimensional stability in contact with molten silicon. These materials may find application as containers and/or shaping dies in processes such as edge-defined film growth.

This paper describes the development and evaluation of proprietary coatings of pure silicon carbide, silicon nitride and aluminum nitride on less pure hot pressed substrates of the respective ceramic materials. Silicon sessile drop experiments were performed on coated test specimens under controlled oxygen partial pressures. X-ray diffraction and SEM characterization was performed prior to testing. The reaction interfaces were characterized after testing with optical and scanning electron microscopy and Auger electron spectroscopy.

Increasing the oxygen partial pressure was found to increase the molten silicon contact angle, apparently because adsorbed oxygen lowers the solid-vapor interfacial free energy. Adsorbed oxygen was also found to increase the degree of attack of molten silicon upon the chemical vapor deposited coatings.

Prototypic containers and dies were delivered and cost projections show that reasonably priced, coated, molten silicon resistant refractory material shapes are obtainable.

TABLE OF CONTENTS

Section		Page
	TECHNICAL CONTENT STATEMENT	i
	ACKNOWLEDGEMENT	ii
	ABSTRACT	iii
	TABLE OF CONTENTS	iv
	LIST OF TABLES	vi
	LIST OF FIGURES	viii
1.	INTRODUCTION	
1.1	SCOPE OF WORK	1
1.2	PROGRAM ORGANIZATION	2
1.3	MATERIALS SYSTEMS INVESTIGATED	5
2.	TECHNICAL DISCUSSIONS	7
2.1	CHARACTERIZATION OF STARTING MATERIALS	7
2.2	HOT PRESSED CERAMIC SUBSTRATES FOR CNTD COATING APPLICATION	7
2.3	CHARACTERIZATION OF CNTD COATINGS	10
2.3.1	Candidate Material System No. 1-CNTD SiC	10
2.3.2	Candidate Material System No. 2-CNTD Si_3N_4	15
2.3.3	Candidate Material System No. 3-CNTD AlN	17
2.3.4	Candidate Material System No. 4-Altered Si_3N_4	19
2.4	CHARACTERIZATION OF LIQUID SILICON-SPECIMEN REACTIONS UNDER PRECISELY CONTROLLED ATMOSPHERES	23
2.4.1	Experimental Procedure	25
2.4.2	Sessile Drop Experiments	30
2.4.3	Microscopic Examination of Sessile Drop Test Specimens	34
2.4.4	Auger Analysis	47
2.4.5	Separation of CNTD Coatings From Substrates	52
2.4.6	Conclusions	62
2.5	MANUFACTURING OF CONTAINERS AND DIES	63
2.5.1	Fabrication of Containers	63
2.5.2	Fabrication of Dies	67

Table of Contents - continued

Section		Page
3.	MANUFACTURING COST PROJECTIONS	75
	3.1 CONTAINER MANUFACTURING PROJECTIONS	
	3.2 DIE MANUFACTURING PROJECTIONS	79
4.	CONCLUSIONS	82
5.	RECOMMENDATIONS FOR FUTURE WORK	85
	APPENDICES	
	APPENDIX A - General Appearance Observations and X-Ray Diffraction Results for Coatings	
	APPENDIX B - Detailed Discussion of the X-Ray Diffraction Characterization of the Altered Si_3N_4 Coating (CMS-4A and 4B)	
	APPENDIX C - Process Specifications	

LIST OF TABLES

Table		Page
I.	Coating/Substrate Candidate Materials Systems Investigated	6
II.	Raw Materials Sources and Vendor's Specifications	8
III.	Semiquantitative Spectrographic Analysis of Metallic Impurities (ppm), Raw Materials	9
IV.	Uncoated Specimen Density and Disposition	11
V.	Container Manufacturing Capital Equipment Requirements	80
VI.	Container Manufacturing Cost Summary	81
VII.	Die Manufacturing Capital Equipment Requirements	83
VIII.	Die Manufacturing Cost Summary	84
A-1.	General Appearance Observations and X-Ray Diffraction Results, CNTD SiC Coatings on SiC (w/1 wt% B) Substrates (CMS-1)	A-1
A-II.	General Appearance Observations and X-Ray Diffraction Results, CNTD Si_3N_4 Coatings on Si_3N_4 (w/4 wt% MgO) Substrates (CMS-2A)	A-3
A-III.	General Appearance Observations and X-Ray Diffraction Results, CNTD Si_3N_4 Coatings on Si_3N_4 (w/4 wt% MgO) Substrates (CMS-2B)	A-5
A-IV.	General Appearance Observations and X-Ray Diffraction Results, CNTD AlN Coatings on AlN Substrates (CMS-3)	A-7
A-V.	General Appearance Observations and X-Ray Diffraction Results, Altered Si_3N_4, Si_2ON_2 Attempt, on Si_3N_4 (w/10 wt% Y_2O_3) Substrates, (CMS-4A)	A-8

LIST OF TABLES - CONTINUED

Table		Page
A-VI.	General Appearance Observations and X-Ray Diffraction Results, Altered Si_3N_4, SiAlON Attempt, on Si_3N_4 (w/10 wt% Y_2O_3) Substrates, (CMS-4B)	A-8
B-I.	Calculated and Experimental Intensities (CMS-4)	B-4
B-II.	Ratios of (222) Peak Intensities to Five Strong Peaks	B-6
C-I.	Parameters for Hot Pressing of Ceramic Substrates	C-4

LIST OF FIGURES

Figures		Page
1.	Technical Aspects of Eagle-Picher/UMR/Chemetal Program	4
2.	CNTD SiC, as Deposited	13
3.	Fractured Surface of CNTD SiC Coating on Hot Pressed SiC	13
4.	Details of CNTD SiC Coating Microstructure on Polished and Etched Surface	14
5.	CNTD Si_3N_4 Coating on Hot Pressed Si_3N_4 (w/4 wt% MgO), Candidate Materials System No. 2, Polished Surface	16
6.	Fracture Surface of CNTD Si_3N_4 Coating on Hot Pressed Si_3N_4 (w/4 wt% MgO), Candidate Materials System No. 2.	18
7.	Scanning Electron Photomicrograph of CMS-4B Coating Containing both Crystalline and Amorphous Phases	22
8.	Scanning Electron Photomicrograph of CMS-4B Coating, Fractured Surface	24
9.	CNTD SiC on Hot Pressed SiC	26
10.	Indirect Contact Angle Measurement Assuming Spheroidal Cap of the Silicon Drop	29
11.	Molten Silicon Contact Angle on CNTD SiC as a Function of Time and P_{O_2}	31
12.	Molten Silicon Contact Angle on CNTD Si_3N_4 as a Function of Time and P_{O_2}	32
13	Molten Silicon Contact Angle on CNTD AlN as a Function of Time and P_{O_2}	33
14.	Interface Between Molten Silicon and CNTD SiC Annealed at 1430°C and 1.8×10^{-20} atm P_{O_2}	35

LIST OF FIGURES - continued

Figures		Page
15.	Relative Positions of Original Silicon Cube, Silicon Sessile Drop, and Specimen	37
16.	Two Configurations for Silicon Cube Placement on Specimen	38
17.	Slicing of Post Sessile Drop Specimen to Characterize Silicon - CNTD SiC Interface at Various Positions	39
18.	Post Sessile Drop Test Specimens of CNTD SiC	41
19.	Molten Silicon - CNTD SiC Interface to Investigate Effects of Tilt Configuration	42
20.	Singular Reaction Point for Tilt Configuration Experiment on CNTD SiC	43
21.	Typical Scanning Electron Micrograph of Clean Portion of Molten Silicon - CNTD SiC Interface	44
22.	Molten Silicon - CNTD Si_3N_4 Interface, Tilt Configuration	45
23.	Comparison of Degree of Molten Silicon Attack of Hot Pressed and CNTD Si_3N_4	46
24.	AES Analysis of CNTD SiC Prior to Sessile Drop Test	48
25.	AES Analysis of CNTD AlN Prior to Sessile Drop Test	49
26.	Post Sessile Drop Auger Electron Surface Analysis, CNTD AlN	50
27.	Auger Electron Analysis of Silicon Drop Melted on CNTD AlN	53
28.	AES on Interface of Silicon and CNTD AlN Before Sputtering	56

LIST OF FIGURES - continued

Figures		Page
29.	Scanning Electron Photomicrograph of CNTD Si_3N_4 - Hot Pressed Specimen Interface After Sessile Drop Testing	58
30.	Separation of CNTD Si_3N_4 Coating From Hot Pressed Substrate	59
31.	Separation of CNTD SiC Coating from Hot Pressed Substrate	59
32.	Scanning Electron Photomicrograph of Reverse Side of a Separated CNTD Si_3N_4 Coating	60
33.	Scanning Electron Photomicrograph of the Reverse Side of a Separated CNTD SiC Coating	61
34.	Hot Pressed Ceramic Container Design	65
35.	CNTD Coated Containers, as Delivered	66
36.	Scanning Electron Photomicrograph of CNTD Si_3N_4 Coating, CMS-2 Container	68
37.	JPL Suggested One Piece Die Design	69
38.	JPL Suggested Two Piece Die Design	70
39.	Eagle-Picher Modified Two Piece Die Design	72
40.	CNTD SiC Coated SiC (w/1 wt% B) Two Piece Die, Assembled	76
41.	Container Manufacturing Process	78
B-1.	Laue Camera Experimental Set-up for Investigating Possible Orientation in the CMS-4 Coatings	B-9
C-1.	Generalized Hot Pressing Cycle	C-4
C-2.	Eagle-Picher Modified Two Piece Die Design, with Surfaces Marked for Grinding Sequence	C-6

1. INTRODUCTION

1.1 SCOPE OF WORK

The JPL Low-Cost Silicon Solar Array Project objective of lowering the cost of silicon photovoltaic material requires the development of refractory materials which exhibit improved chemical and dimensional stability in contact with molten silicon. These materials find application as containers and/or shaping dies in processes such as edge-defined film growth (EFG). The performance of these materials has a direct impact upon the cost per unit area of silicon by virtue of equipment throughput between replacement of critical items. Refractory material performance, in addition, is a determinator of the chemical and structural quality of the silicon ribbon obtained, and therefore of cell efficiency.

This program was designed to develop and evaluate refractory materials which would attempt to meet the following requirements:

a) The material must be mechanically stable to temperatures greater than the melting point of silicon (1412^{0}C). Thus, it must not melt or undergo other destructive phase changes below this temperature.

b) Materials in contact with molten silicon must be dimensionally stable, to 0.5 mil over a 24 hour period in the case of dies. This is necessary to maintain dimensional control of the processed silicon strip, and is to include erosion, corrosion, or growth of surface reaction products. With container materials, acceptable reaction rates will be controlled by permissible impurity level.

c) The die and container material must not excessively contaminate silicon processed through it. Present indications

suggest that 10^{15} atom/cc is an upper limit for general impurities. Exceptions to this are: aluminum, phosphorus, boron, arsenic, and gallium, which may be present one or two orders of magnitude higher, and carbon, oxygen, and nitrogen, which may be present in amounts dictated by erosion rates (approximately 10^{19} atoms/cc). However, revision of these numbers may occur as knowledge of their specific effects is developed. For example, there are indications that structural imperfections result from carbon levels greater that 1×10^{18} atom/cc.

d) The process or processes developed must be amenable to the fabrication of dies and containers with close tolerances and varying geometries.

e) The die to be produced and evaluated on this program shall be capable of producing and maintaining a capillary column of silicon 1 to 3 cm. wide x 0.01 cm. thick to a height of at least 2.5 cm. Experience with other materials has indicated that a contact angle of less than 80° is required.

1.2 PROGRAM ORGANIZATION

The program was organized as a cooperative effort among three facilities to develop successful die and container materials for handling liquid silicon while it is being formed into photovoltaic cell material and determine the effects of oxygen partial pressure upon material performance. Overall project management as well as die and container fabrication and characterization were provided by the Miami Research Laboratories (MRL) of Eagle-Picher Industries, Inc. Chemetal Corporation (Pacoima, California) applied ceramic coatings to substrates made by MRL

for sessile drop testing and later to die and container shapes also made by MRL. All coatings were applied using the Chemetal proprietary CNTD* process. University of Missouri-Rolla (UMR) personnel performed sessile drop experiments on coated substrates made by MRL and Chemetal. They explored the effects of oxygen partial pressure and characterized the reactions using Auger electron spectroscopy and scanning electron and optical microscopy.

The technical aspects of the program are delineated in Figure 1. Ceramic bodies fabricated from powders generally contain secondary grain boundary phases which, in many applications, degrade the ultimate thermodynamic stability of the pure material. These phases are often the "weak link" whereby corrosive or reactive species are able to compromise the integrity of the body. The application of the ceramic coating from the vapor phase without the intentional addition of secondary phases was utilized to provide a test of the ultimate potential of the materials in molten silicon handling applications.

It is important that the coefficient of thermal expansion of the substrate be closely matched to that of the coating in order to maintain coating integrity during cool down after CNTD deposition and during testing or use. For this reason the coatings were applied to substrates of ceramic bodies of the same nominal chemical composition fabricated from powders by the addition of minor ($\leq$ 4 wt %) additives.

The investigation of the effects of oxygen partial pressure was undertaken to determine what use conditions would enhance the resistance of these refractory ceramic materials to attack by molten silicon.

---

* CNTD is a Chemetal Corp. acronym for their proprietary dense CVD (Chemical Vapor Deposition) coating. The letters stand for Controlled Nucleation Thermal Deposition.

1. COATINGS OF PURE CERAMIC MATERIALS W/O FABRICATION ADDITIVES

2. COMPATIBLE SUBSTRATES OF LIKE CERAMIC FABRICATED FROM POWDERS

   A. VERY NEAR MATCH OF COATING/SUBSTRATE COEFFICIENT OF THERMAL EXPANSION

   B. OXYGEN PARTIAL PRESSURE NOT FIXED BY SPECIMEN AS MAY BE THE CASE WITH GRAPHITE SPECIMEN OR HARDWARE

3. INVESTIGATION OF THE EFFECTS OF OXYGEN PARTIAL PRESSURE UPON CONTACT ANGLE AND MOLTEN SILICON COMPATIBILITY VIA SESSILE DROP TESTING

4. CHARACTERIZATION BEFORE AND AFTER SESSILE DROP TESTS

5. DIE AND CONTAINER DELIVERY TO JPL

FIGURE 1

TECHNICAL ASPECTS OF EAGLE-PICHER/UMR/CHEMETAL PROGRAM

The relative resistance to attack by molten silicon was studied by characterization of the coatings before, and the silicon - coating interface after, sessile drop testing. The effect of oxygen partial pressure upon the molten silicon contact angle, ie. wettability, has important ramifications when these materials are employed to grow silicon ribbons by capillary rise through a die.

1.3 MATERIALS SYSTEMS INVESTIGATED

During the conception of this program the literature pertaining to molten silicon-refractory materials compatibility was surveyed. While the referenced report* was not available at that time, it is recommended for its experimental findings and literature references.

Four candidate materials systems (CMS) were selected for investigation in the Eagle-Picher/Chemetal/UMR Program. The CMS's 1, 2, and 4 were chosen by virtue of the incorporation of a noncontaminating cation (Si) and the potential shown in previous investigations of these materials fabricated by conventional means. The CMS-3 choice was based upon the thermodynamic stability of AlN and the absence of definitive previously existing data. The coating/substrate candidate materials systems investigated are summarily described in Table I. The four systems were evaluated by sessile drop screening tests at UMR and two very promising systems, no. 1 and no. 2-A, were chosen for die and container hardware delivery.

The detailed characterization of starting materials, substrates, coatings and molten silicon interfacial phenomena are found in section 2, Technical Discussions.

---

* T. O'Donnell, M. Leipold, and M. Hagan, Compatibility Studies of Various Refractory Materials in Contact with Molten Silicon, JPL Publication 78-18.

TABLE I

Coating/Substrate Candidate Materials Systems Investigated

CANDIDATE MATERIALS SYSTEM NUMBER	HOT PRESSED SUBSTRATE	PURE CNTD COATINGS
1	SiC w/1 wt% B	SiC
2-A	Si_3N_4, 95-98% pure (RM-3),[1] w/4 wt% MgO	Si_3N_4
2-B	Si_3N_4, 99.9% pure (RM-4), w/4 wt% MgO	Si_3N_4
3	AlN	AlN
4-A	Si_3N_4 (RM-5) w/10 wt% Y_2O_3	Si-O-N[2]
4-B	Si_3N_4 (RM-5) w/10 wt% Y_2O_3	Si-Al-O-N[2]

1. RM - no.'s refer to Table II

2. Structural modifications of Si_3N_4 planned by introduction of aluminum and/or oxygen bearing gases into the reaction/deposition system. See section 2.3.4 for results.

2. TECHNICAL DISCUSSIONS

2.1 CHARACTERIZATION OF STARTING MATERIALS

The complete control of bulk and grain boundary impurities in fabricated ceramic articles is difficult to achieve in practice. Quite often one finds that powders of the desired purity are not commercially available. When the system under consideration is a nitride or carbide ceramic, oxygen is a common impurity, and a thorough powder characterization must include an analysis of both the cation and the anion species. One of the key aspects of our program was the application of pure ceramic coatings as barriers to molten silicon penetration and this obviated the requirement for detailed chemical analysis of the underlying substrates.

Emission spectroscopy was performed on all powders. The vendor's of the various powders are identified and their advertised specifications are shown in Table II. The results of semiquantitative emission spectroscopy analysis are shown in Table III. The powders, with the appropriate additives, could be hot pressed to adequate density; therefore particle size and BET data were not obtained.

2.2 HOT PRESSED CERAMIC SUBSTRATES FOR CNTD COATING APPLICATION

The hot pressed ceramic substrates were coated with CNTD ceramic materials prior to sessile drop testing. This section will briefly describe their manufacture, however, a complete treatment can be found in the Process Specifications in the Appendices.

The starting powders were mixed with the appropriate pressing additives in aqueous or organic vehicle slurries either by high speed, high shear blending in a Waring laboratory blender or by wet milling in a rubber lined ball mill with steel balls. The slurries were vacuum dried (< 1 mm Hg) above 100°C for at least 1 hour. The

TABLE II

Raw Material Sources and Vendor Specifications

RAW MATERIAL NUMBER	DESCRIPTION	VENDOR	VENDOR'S SPECIFICATIONS
RM-1	SiC-Silcar N	Elecktroschmelzwerk-Kempton	90-95% SiC, 3% SiO_2, 1% free C; 0-15μ grain dist.
RM-2	B	Callery Chemical Co.	99.99% pure on metal basis, amorphous, submicron
RM-3	Si_3N_4-No. 1159 Commercial Grade	Cerac Inc.	95-98% Si_3N_4, 1-3% free Si, 0.5-0.9% O; 100% β; 1-3μ avg.
RM-4	Si_3N_4-No. 1481 Electronic Grade	Cerac Inc.	99.9% pure on metal basis, 99.1% Si+N; 100% β; 1-3μ avg.
RM-5	Si_3N_4- Controlled Phase 85	Kawecki Berylco Ind.	97.4% Si+N, 0.55% O; min. 85% α; -325 mesh
RM-6	AlN	Elecktroschmelzwerk-Kempton	97.5% Al+N; 3-10μ avg.
RM-7	MgO	Aremco Products, Inc.	99.9% pure on metal basis 1-5μ avg.
RM-8	Y_2O_3-No. 5600	Molycorp	99.99% pure on metal basis 1-5μ avg.

TABLE III

Semiquantitative[1] Spectrographic Analysis[2] of Metallic Impurities (ppm), Raw Materials

Impurity	SiC RM-1	B RM-2	Si_3N_4 RM-3	Si_3N_4 RM-4	Si_3N_4 RM-5	AlN RM-6	MgO RM-7	Y_2O_3 RM-8
Al	2000	*	20000	1000	2000	major	10	5
B	5	major	10	30	10	100	50	*
Ca	30	*	2000	20	30	20	1000	5
Cr	10	*	1000	10	500	40	100	5
Cu	20	6.5	30	5	30	20	10	<5
Fe	3000	*	3000	10	3000	10000	1000	*
Mg	20	6.4	100	10	20	50	major	1
Mn	30	*	10	3	50	50	30	.5
Mo	*	*	*	*	1000	*	*	*
Na	100	*	*	*	*	*	*	*
Ni	500	*	50	*	500	10	20	*
Si	major	30	major	major	major	500	5000	10
Sn	5	*	10	*	10	*	5	5
Ti	500	*	500	20	500	*	80	*
V	1000	*	3	*	*	*	*	*
Zn	30	*	30	*	30	*	*	100

* None detected

1. Full quantitative analysis would require standards for each impurity element.

2. All analysis reported here were performed at the Miami Research Laboratory, on a Jarrell-Ash Mark IV Emission Spectrograph.

dried slurry cakes were delumped in an Al_2O_3 or glass mortar and pestle followed by 5 minutes milling in a Spex Shatterbox mill (steel), and stored in polyethylene jars.

The powder was loaded into graphite tooling and hot pressed to greater than 90% theoretical density (T.D.) in all cases, and normally to greater than 95% T.D. The specimens were initially ground to 1.2" dia x 0.16" thickness using a 100 grit diamond wheel. The specimen diameter was soon changed to 1.05" to facilitate sessile drop testing, however, the first specimens were used without reworking in any way. A summary of the specimen densities and their disposition to the candidate materials systems is shown in Table IV.

2.3 CHARACTERIZATION OF CNTD COATINGS

The specimen characterization efforts were concentrated on the CNTD coatings because these coatings were to be in direct contact with the molten silicon. The techniques of optical and scanning electron microscopy and x-ray diffraction were utilized in characterization. Some x-ray diffraction characterization was also performed on the hot pressed substrates. The diffraction patterns showed the substrates to be much like the beginning powders in phase content, although some conversion of alpha to beta Si_3N_4 was observed for the discs pressed from the higher alpha content Si_3N_4 powder. The discussion of CNTD coating characterization follows.

2.3.1 Candidate Material System No. 1 - CNTD SiC

The as-deposited surfaces of the CNTD SiC coatings had a reasonably uniform general appearance, although some degree of variation with

TABLE IV

Uncoated Specimen Density and Disposition

Chief Constituent	Pressing Additive	Average Lot Density[1]	CMS[2] Substrate Disposed to
SiC (RM-1)	1 wt% B (RM-2)	3.02 g/cm^3 (94.9%TD)	CMS-1
Si_3N_4 (RM-3)	4 wt% MgO (RM-7)	3.10 g/cm^3 (96.8%TD)	CMS-2A
Si_3N_4 (RM-4)	4 wt% MgO (RM-7)	3.16 g/cm^3 (98.8%TD)	CMS-2B
AlN (RM-6)	None	3.12 g/cm^3 (95.7%TD)	CMS-3
Si_3N_4 (RM-5)	10 wt% Y_2O_3 (RM-8)	3.16 g/cm^3 (95.8%TD)	CMS-4A & 4B

1. As hot pressed and ground, before coating
2. Candidate Materials System (see Table I)

respect to reflectivity and smoothness did exist. (see Table A-I of Appendix A) The coating appeared nodular when observed at low magnifications but with evidence of a much finer substructure. The substructure is discernable in the SEM photomicrograph, Figure 2. Figure 3 shows a fractured surface of the same specimen with an apparent columnar structure in the coating, parallel with the direction of growth. Careful examination of the photograph reveals fine relief on the larger, relatively smooth surfaces.

Polished sections of the coating material were prepared and etched electrolyticly and thermally. A one hour thermal etch in flowing argon at 1400°C was reasonably effective in revealing the ultimate microstructure of the coating. The action of the thermal etch was not uniform across the sample as shown in Figure 4-a. Silicon maps were made by Energy Dispersive X-Ray Analysis and the silicon content was not found to vary, beyond the detection limits, between the more readily etched and the less readily etched regions. No appreciable difference in background elements was detected.

The potential of the CNTD process for depositing fine grained coatings is shown in Figure 4-b, where grains as small as 0.25μ (2500 Å) are revealed. The boundaries between the etched and unetched regions do not indicate that the unetched regions are large crystallites. The coating appears to consist of regions or zones of varying growth orientation or structural polytype with extremely fine grains on a local basis. The CNTD SiC deposits were free of cracks and polished sections were free of porosity.

The x-ray diffraction analysis of the coatings is summarized in Table A-I of Appendix A. The diffraction patterns were generally consistent.

Figure 2. CNTD SiC Coating, as Deposited

Indicates fine grain substructure, SEM, 600X.

Coating

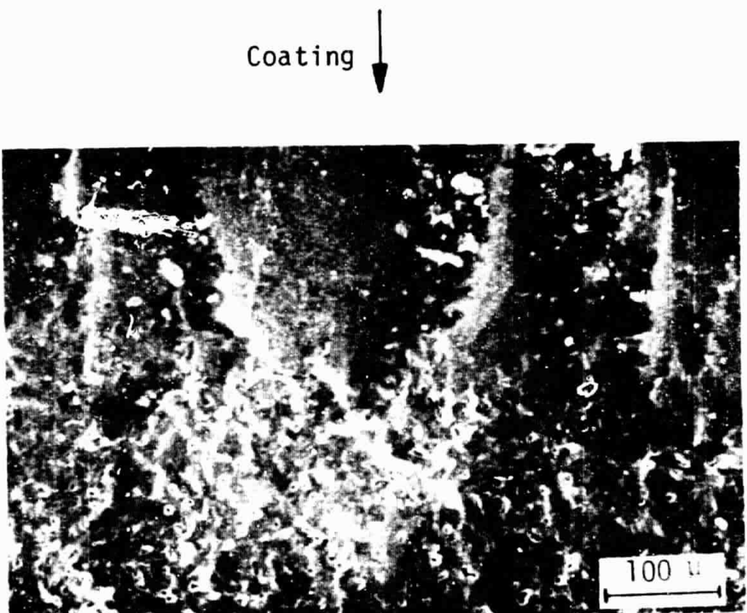

Hot Pressed Substrate

Figure 3. Fractured Surface of CNTD SiC Coating on Hot Pressed SiC

Regions of finer structure between apparent columns, SEM, 160X.

a)

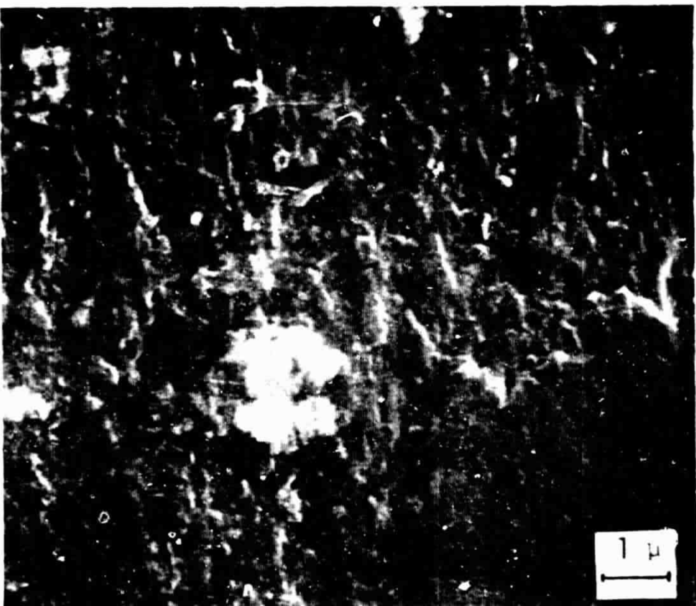

b)

Figure 4. Details of CNTD SiC Coating Microstructure on Polished and Etched Surface

a) Nonuniform etching, (1400°C, 1 hr. flowing Ar), 600X
b) Resolution of fine grained region, 9000X

All coatings were crystalline β-SiC. Several peaks showed broadening indicative of fine particle size and the 222 peak was extremely intense, indicative of preferred orientation or structure factor changes due to nonstoichiometry.

2.3.2 Candidate Materials System No. 2 - CNTD Si_3N_4

The Candidate Materials System No. 2 consisted of two subgroups. The subgroups were designated by virtue of the intentional variation of the purity of the hot pressed Si_3N_4 (4 wt% MgO) substrates between subgroups. The substrate differences were determined to impart no discernable difference to the CNTD Si_3N_4 coatings. The specimen to specimen coating variations were attributable to CNTD process variations in the optimization of the coating, rather than substrate purity.

The CNTD Si_3N_4 coatings were of two general types, amorphous and crystalline. The amorphous coatings were translucent yellow, green, or variegations thereof. The crystalline coatings were similarly (but less intensely) colored, in general translucent, tending toward transparency. Each subgroup, CMS 2-A and 2-B, consisted of approximately one-third totally or partially amorphous coatings with the remaining two-thirds of the specimens being totally crystalline.

The translucent coatings exhibited crack-like macrostructures, but nearly all of the systems ended within the coatings. Only a few appeared to come through to the surface. The photomacrograph in Figure 5-a shows the crack-like network on a polished specimen. The larger magnification photo 5-b shows that the apparent cracks normally terminate below the surface. Polishing flaws at the surface are in sharp focus while the apparent cracks are below the depth of field of the microscope and are therefore out of focus. These details would have been in sharp focus had they propagated to the surface.

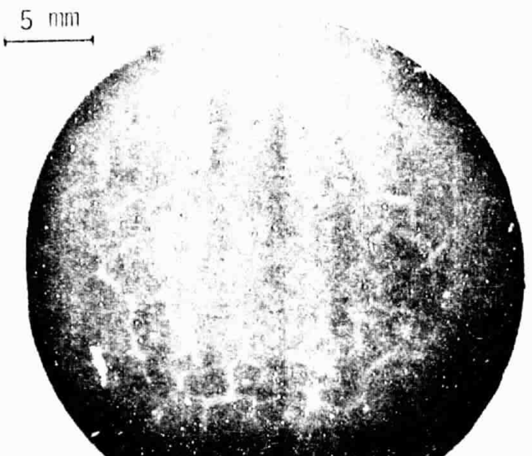

a) 2.44X

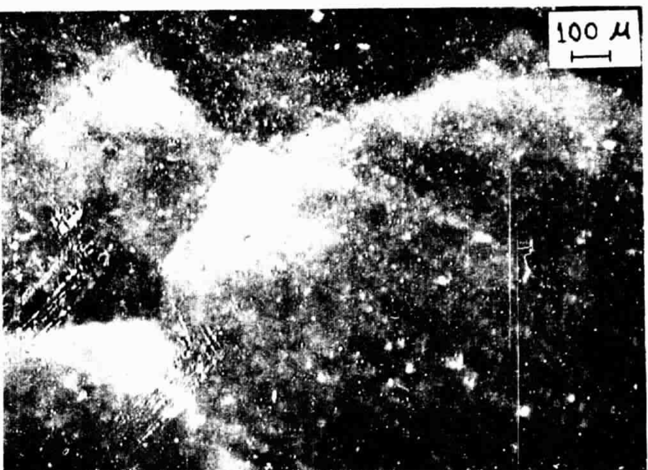

b) 52.5X

Figure 5. CNTD Si_3N_4 Coating on Hot Pressed Si_3N_4 (w/4 wt% MgO), Candidate Materials System No. 2, Polished Surface

The microstructural information obtained for the CNTD Si_3N_4 coatings was observed on fractured specimens. These coatings appeared extremely dense. Figure 6-a shows the CNTD structure at 2000X and suggests a grain size on the order of 20 to 25 μ. A larger magnification (Figure 6-b) reveals grains on the order of 1 μ or less, demonstrating the capability of CNTD fabrication to produce reasonably fine grained Si_3N_4.

The atomic structure of the CNTD Si_3N_4 coatings was investigated by in situ x-ray diffraction of the coated surfaces. The results are shown in Table A-II and Table A-III in the Appendices. The coatings were, as mentioned, of two basic types, crystalline and amorphous. The crystalline coating diffraction patterns indicate essentially α-phase Si_3N_4 with some doubtful β-phase. The relative intenity values varied from specimen to specimen indicating possible orientation effects, or structure factor changes due to nonstoichiometry or disordering.

2.3.3 Candidate Material System No. 3 - CNTD AlN

The AlN powder from which the hot pressed substrates were fabricated (RM-6, Table II) was found to contain 10,000 ppm of iron. X-ray diffraction patterns from the powder and from the hot pressed substrates showed eight minor peaks of one or more secondary phases.

Based upon the high iron content and the expected presence of oxygen or free aluminum, an effort was made to rationalize the unknown minor peaks of the diffraction pattern to the expected peaks of twenty-nine crystal structures, including ten phases of Al_2O_3, three iron aluminum intermetallics and elemental aluminum and iron. None of these compounds could be rationalized with the eight minor peaks.

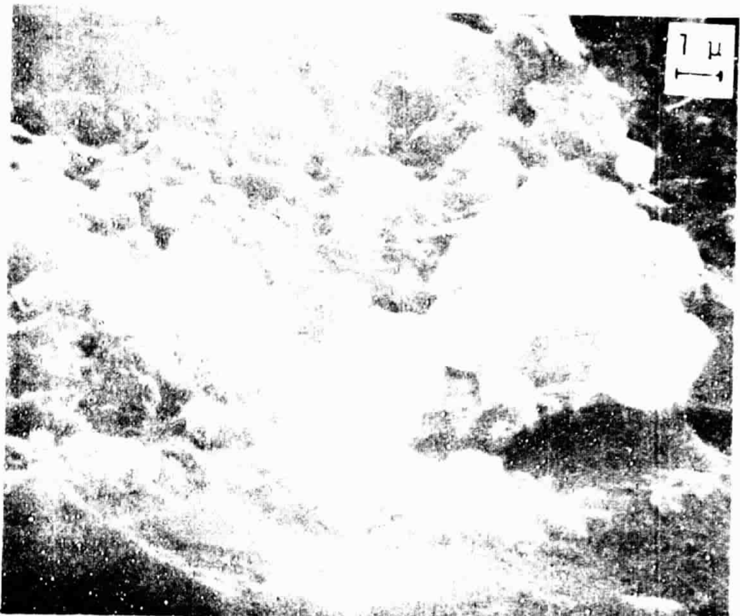

a) - 2000X

b) - 6000X

Figure 6. Fractured Surface of CNTD Si_3N_4 Coating on Hot Pressed Si_3N_4 (w/4 wt% MgO), Candidate Materials System No. 2.

Shows variances in texture from moderate to extremely fine grained, all coating.

The CNTD AlN coated surfaces were found to be crystalline, single phase, hexagonal AlN. No amorphous tendencies were observed. The minor unidentified peaks which had been observed in the powder and in the hot pressed body were much weaker or absent in the patterns obtained from the coatings. Several coatings did exhibit very minor peaks at up to three of the eight suspect positions indicating there was some tendency for the impurity (ies) to "bleed through".

The relative peak heights observed in the patterns obtained from the CNTD AlN coatings were not in the same ratios as those given in the ASTM card file, although the peak positions were correct. This is not surprising for a CVD type coating, and has been attributed to orientation effects, or structure factor changes.

The 100 peak was consistently low and the 101, 102, 103, 112, and 203 peaks were consistently high. The orientation of the deposited crystallites and/or other factors affecting peak height are thus assumed to be consistent from specimen to specimen.

A summary of the Chemetal observations and MRL x-ray diffraction results are shown in TABLE A-IV of the Appendices.

2.3.4 Candidate Material System No. 4 - Altered Si_3N_4

The coatings were deposited by the proprietary Chemetal process, similar to the CNTD Si_3N_4 but with the introduction of oxygen and/or aluminum bearing gases during the deposition process. Two types of altered Si_3N_4 structures were taken under development. The first (CMS-4A) was an attempt to introduce oxygen into the Si_3N_4 crystal lattice and form Si_2ON_2. The second was an attempt to introduce oxygen and aluminum into the lattice and form silicon nitride polymorphs in the SiAlON system.

The X-ray diffraction data shows that the hopes of depositing Si_2ON_2 (CMS-4A) and SiAlON (CMS-4B) were not realized. The X-ray diffraction results are summarized in Tables A-V and A-VI of the Appendices. The deposits were crystalline α-Si_3N_4, except in those cases where they were partially or totally amorphous. No Si_2ON_2 peaks were found in CMS-4A and no d-spacing (angular peak position) changes associated with SiAlON phases were detected for CMS-4B coatings.

These coatings were analyzed on the diffractometer at two settings of the detector sensitivity, without demounting the specimen to facilitate relative intensity comparisons for peaks of widely varying height. The determination of phases present was relatively straightforward. The major complication was a slight angular shift of peak position which was determined by analysis of the same coatings on another machine to be due to mechanical problems related to the sample holder.

The analysis of relative intensities was considerably more difficult. Variations from the expected powder diffraction values of up to 1000% were observed The detailed discussion of these results are found in Appendix B. These intensity variations could be explained by an oriented growth pattern, a non-uniformity of crystallite size, a change in the structure factor due to nonstoichiometry, limited incorporation of Al and/or O atoms into the α-Si_3N_4 structure as interstitials or as substitutions for Si and N respectively, or any combination of these.

The work done at MRL and at Pittsburg State University, Pittsburg, Kansas, (Appendix B) indicates that while preferred orientation cannot be ruled out, it did not exist in strong degree. The Laue back reflection

experiments did indicate that the coatings contained crystallites in the range of 0.1 mm to 0.6 mm (100 to 600 μ). The scanning electron microscopic studies confirmed that a wide distribution of grain sizes existed in these coatings. The most probable explanation for the relative intensity variations is the variation in crystallite size, although this could not be demonstrated without removing the coating, grinding to a fine particle size, and comparing powder diffraction patterns to as-deposited patterns. The coatings were tightly adherent and this work could not be performed under the scope of the contract.

The CMS-4A coatings exhibited a relatively coarse crystalline appearance as-deposited. The coatings were translucent with the coloration observed to vary from faint grey to faint tan or a deeper brown from sample to sample but were reasonably uniform across a given sample. They exhibited the network type cracks similar to those found in the CMS-2 CNTD Si_3N_4 coatings. Most of the cracks appeared to terminate within the coating rather than coming through to the polished surface.

The CMS-4B coatings also appeared coarsely crystalline as-deposited. Figure 7 is a scanning electron photomicrograph of a coating shown by X-ray diffraction to be partly crystalline and partly amorphous. The crystalline region is readily apparent. The botryoidal regions may contain the amorphous phase although this was not verified. The specimen was also examined by EDX analysis to check for Al which might be contained in the lattice below the level of X-ray diffraction detectability, however, nothing above background was indicated. This data again verifies that no appreciable SiAlON phase was formed in the deposited coating.

Figure 7. Scanning Electron Photomicrograph of CMS-4B Coating containing both Crystalline and Amorphous Phases

The CMS-4B coating group showed less tendency to crack and they were in general translucent to opaque. The color varied from light tan to dark brown and nearly black. The grain structure of the CMS-4B coatings was studied on fractured surfaces with the SEM. Some results are shown in Figure 8. While larger grains apparently coexist with smaller ones, grains as small as 1μ and less are distinguishable in Figure 8-b.

2.4 CHARACTERIZATION OF LIQUID SILICON-SPECIMEN REACTIONS UNDER PRECISELY CONTROLLED ATMOSPHERES

The goal of the program segment carried out at UMR was to evaluate the compatibility of molten silicon with CNTD coated SiC, Si_3N_4, and AlN specimens with the view toward determining which material would have the best properties for use in dies and containers in the production of silicon sheets and ribbons. The properties desired in such materials would: 1) resist any form of attack which would erode the die material (so it could not maintain its dimensions) and 2) preserve the silicon purity. The emphasis was on determining the influence of oxygen partial pressure in the furnace ambient atmosphere on: 1) the molten silicon wetting angle and 2) the microscopic attack of molten silicon on these CNTD coated specimens. These investigations have now been completed.

It has been demonstrated that the degree of attack of molten silicon on the CNTD coated specimens is much less than on uncoated (hot pressed) samples, and that the presence of oxygen is a strong factor influencing this degree of attack. Also, of the three CNTD coated materials tested, SiC appeared to have resistance to attack superior to that of either AlN or Si_3N_4.

a) 500X

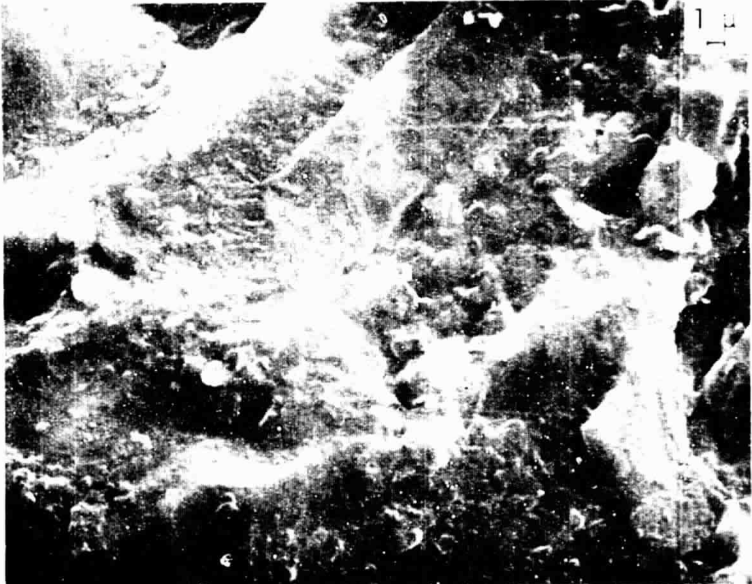

b) 2500X

Figure 8. Scanning Electron Photomicrographs of CMS-4B Coating, Fractured Surface

Both photomicrographs from same region of sample, all coating

Silicon sessile drop experiments were conducted on the CNTD AlN, SiC, and Si_3N_4 coatings to determine the effects of oxygen partial pressure on the wettability of molten silicon with these samples. Characterizing techniques of Optical Microscopy, Scanning Electron Microscopy (SEM) and Auger Electron Spectroscopy (AES) were employed on the post sessile drop test specimens to evaluate the severity of attack of molten silicon on these materials.

It was found that the presence of residual oxygen adsorbed on the surfaces increases the rate of attack of the samples. The exact mechanism has not been investigated.

2.4.1 Experimental Procedure

Hot pressed specimens of SiC, Si_3N_4, and AlN were fabricated by the Miami Research Laboratories of Eagle-Picher Industries, Inc., and then CNTD coated by Chemetal, Corp. The coating on each specimen consisted of essentially the same chemical composition as the hot pressed substrate, deposited by the CNTD process to produce a theoretically dense and fine grain structure. The coated surfaces, however, are not microscopically planar as deposited, the degree of roughness increasing with coating thickness, Figure 9. A diamond polishing process was therefore employed to produce a 15μm flat surface on each specimen. A polished surface was considered desirable for the sessile drop experiments in order that microscopic and macroscopic contact angles be the same and that the surface geometry and condition be constant from specimen to specimen.

The contact angle between molten silicon and a substrate in a sessile drop experiment is a measure of the degree of wetting and is thus an indicator of the relative interfacial free energies and the compatibility

Figure [illegible]. CNTD [illegible] on Hot Pressed SiC
As-deposited, 118X

of the silicon with the substrate material. The contact angles were measured at 1430°C as a function of time and oxygen partial pressure. The interaction of molten silicon with the specimens at temperature was then evaluated after cooling to room temperature by characterizing the post sessile drop test specimens.

All sessile drop experiments were conducted at 1 atmosphere total pressure in a sealed alumina tube under a flowing gas buffer to control the oxygen partial pressure at a predetermined fixed value. The specimens were placed in the hot zone of a molybdenum resistance furnace, and pyrex ultra-high vacuum type viewports, sealed at each end of the alumina tube, allowed simultaneous temperature and silicon sessile drop contact angle measurements to be made. Oxygen partial pressure in the furnace atmosphere was carefully controlled over a range of interest which included the calculated equilibrium partial pressure for the formation of SiO_2 (2×10^{-18} atm). An H_2/H_2O flowing gas buffer system was employed in the oxygen partial pressure control because its range includes these extremely low oxygen partial pressures whereas other buffers such as the CO/CO_2 system do not. A thoria-yttria solid electrolyte oxygen sensor was employed to determine the oxygen partial pressures for the same reason.

Most silicon sessile drop tests were conducted at 1430° ± 10°C which is about 20°C above the melting point of silicon, with occasional experiments made at temperatures of about 1490°C. For each experiment the oxygen partial pressure, P_{O_2}, was held constant within the range 10^{-17} to 10^{-21} atm. Duration of experiments ranged from one to twelve hours. Previous sessile drop measurements in the literature have been limited to relatively short time runs of one hour or less. Longer runs

were considered more meaningful because short time measurements are not only less reproducible but do not represent data of significance for application in actual longer use time, i.e. melting and forming silicon into sheets or ribbons.

Photographs of the molten silicon drops were taken during the tests at appropriate intervals and calculations of the contact angle were made from these photographs. These calculations assume that the drop is part of a sphere, or in other words, the flattening of the drop due to gravity is negligible. This is a fair assumption for the small low-density drops used in this work. (Figure 10)

Post sessile drop specimens were sectioned and polished for microstructural study to observe the degree and nature of the molten silicon attack. SEM examination in the post sessile drop fractured specimens was also employed to elucidate the dimensional stability and the erosion and corrosion reactions.

Auger spectroscopic analysis was conducted on the pre- and post sessile drop test specimens to determine the constituent elements at the surface, and the molten silicon - specimen interface reaction. The post sessile drop test specimen was cut at a small angle with respect to the interface to remove the silicon drop. Grinding and etching with a solution of $3HF:5HNO_3:COOH$ were subsequently employed on a specimen so cut to produce a thin residual silicon layer. The specimen was then placed inside the vacuum chamber of an Auger Spectrometer. Access to the interface was made by sputtering through the silicon layer while Auger analysis was simultaneously being made at the bottom of the crater to determine the degree and nature of the interaction in the interface region.

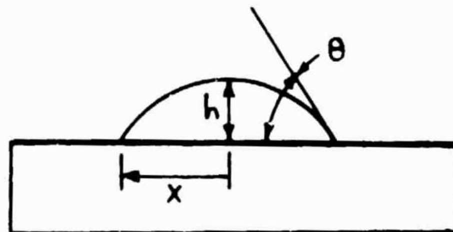

h = height of drop

x = radius of the drop at the basal plane

$\theta = 2 \tan^{-1} (h/x)$

Figure 10. Indirect Contact Angle Measurement Assuming Spheroidal Cap of the Silicon Drop

2.4.2 Sessile Drop Experiments

For the initial sessile drop experiments a silicon cube was placed on the specimen to be tested, which was then placed at the center of the furnace tube and leveled. The flow of the desired experimental atmosphere was then established. Upon melting, the sessile drop contact angle began to decrease, more rapidly at first, tending toward a constant small rate of change after 1 hour.

The effect of changing the oxygen partial pressure is exhibited in figures 11, 12, and 13. It is apparent that the oxygen atmosphere has a marked influence on the ability of silicon to wet these materials, with the contact angle becoming smaller (more wetting) with lower oxygen partial pressure.

The relation of the contact angle to the interfacial energies for a liquid drop on a plane solid surface can be expressed as:

$$\gamma_{LV} \cos\Theta = \gamma_{SV} - \gamma_{LS},$$

where Θ is the contact angle, and γ_{LV}, γ_{SV} and γ_{LS} are the interfacial energies of liquid-vapor, solid-vapor, and liquid-solid interfaces, respectively. When the oxygen partial pressure in the furnace atmosphere increases, the interfacial energy terms of those interfaces which adsorb oxygen from the vapor phase will decrease as more oxygen becomes available. The contact angle Θ is observed to be larger for higher oxygen partial pressures. The surface energy for the solid-vapor interface, γ_{SV}, is believed to be the term most susceptible to the change in oxygen partial pressure. It is noted that there appeared to be a slow but continual decrease in the contact angle even after several hours at temperature.

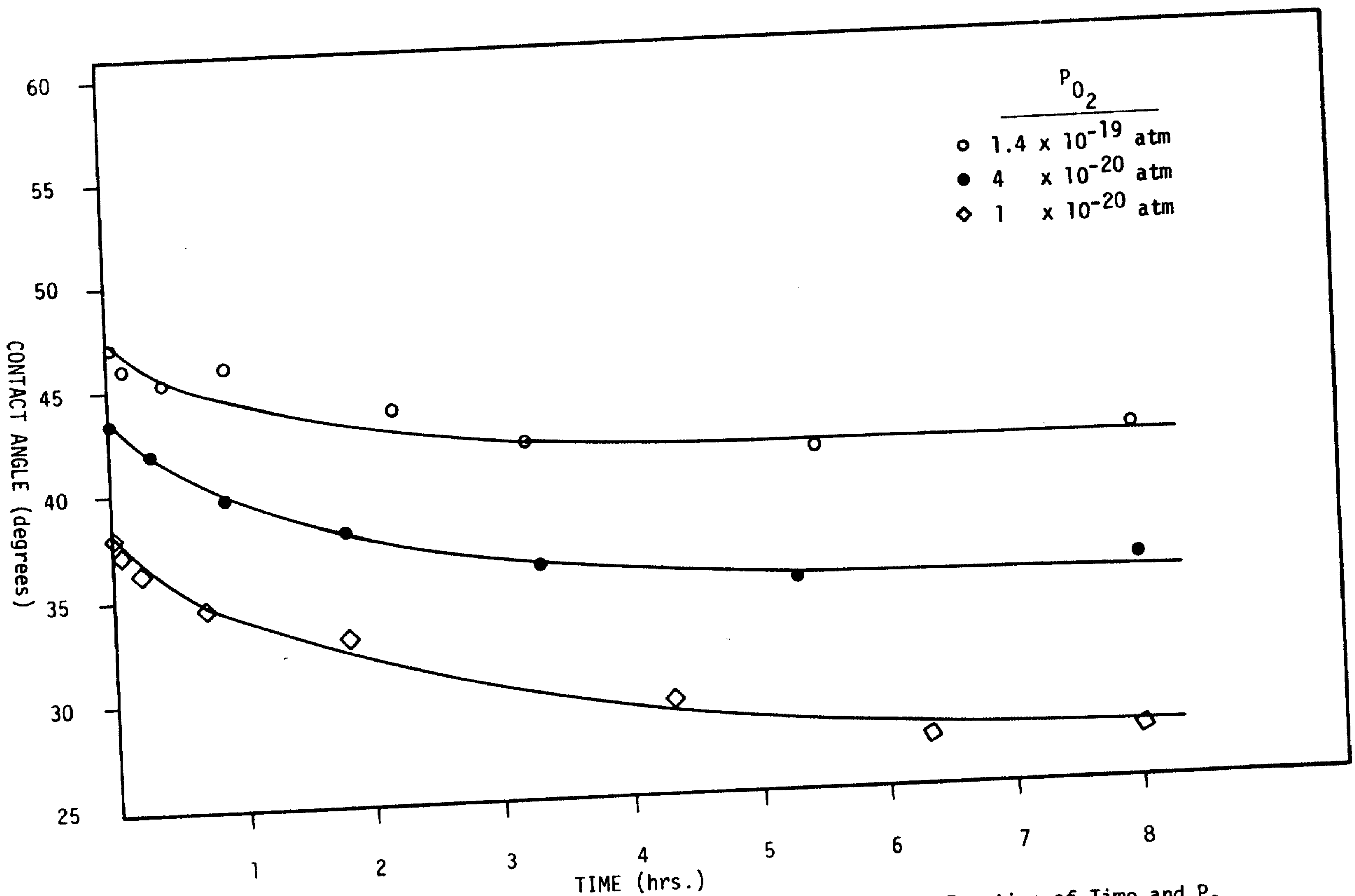

Figure 11. Molten Silicon Contact Angle on CNTD SiC as a Function of Time and P_{O_2}

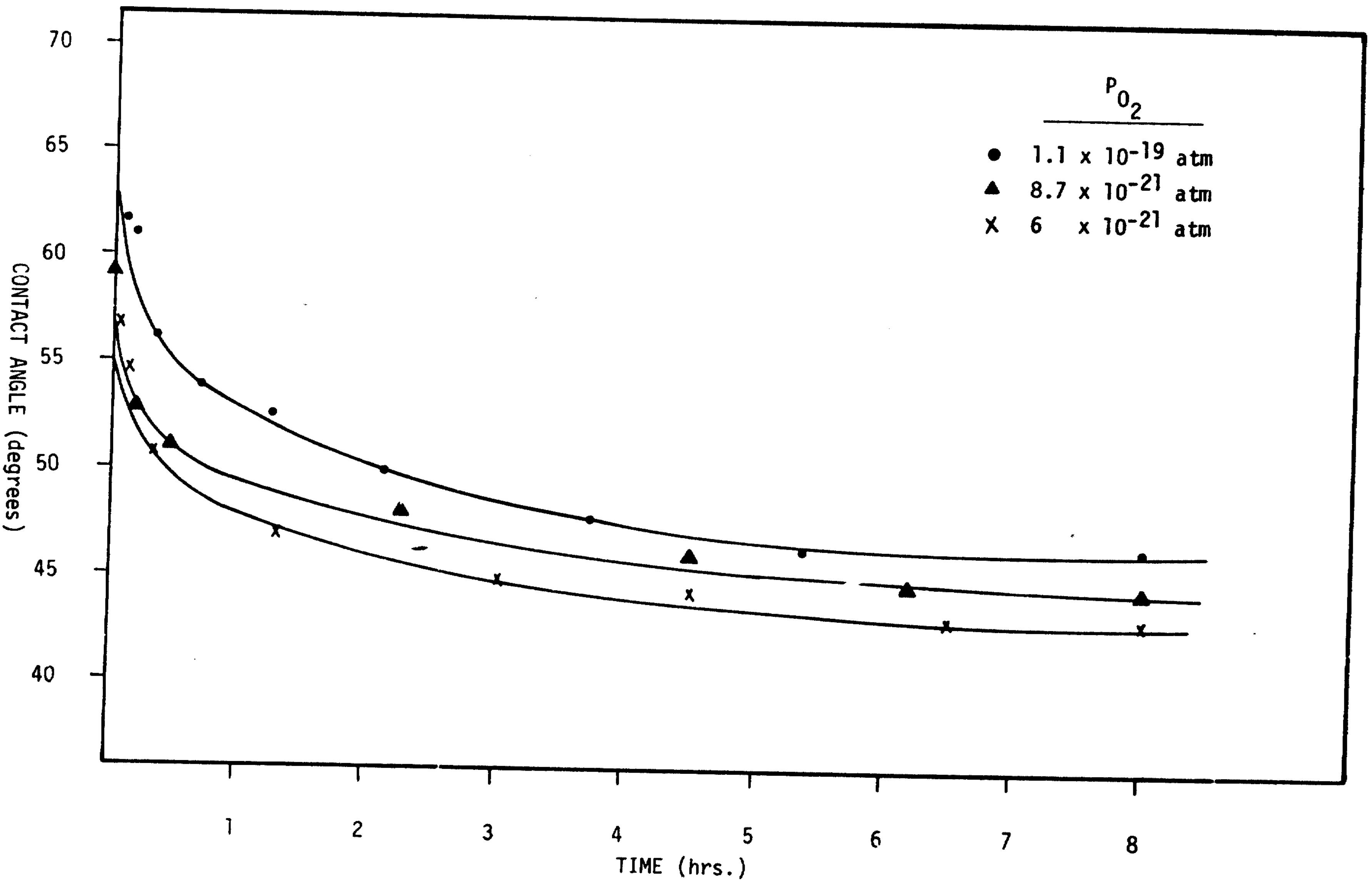

Figure 12. Molten Silicon Contact Angle on CNTD Si_3N_4 as a Function of Time and P_{O_2}

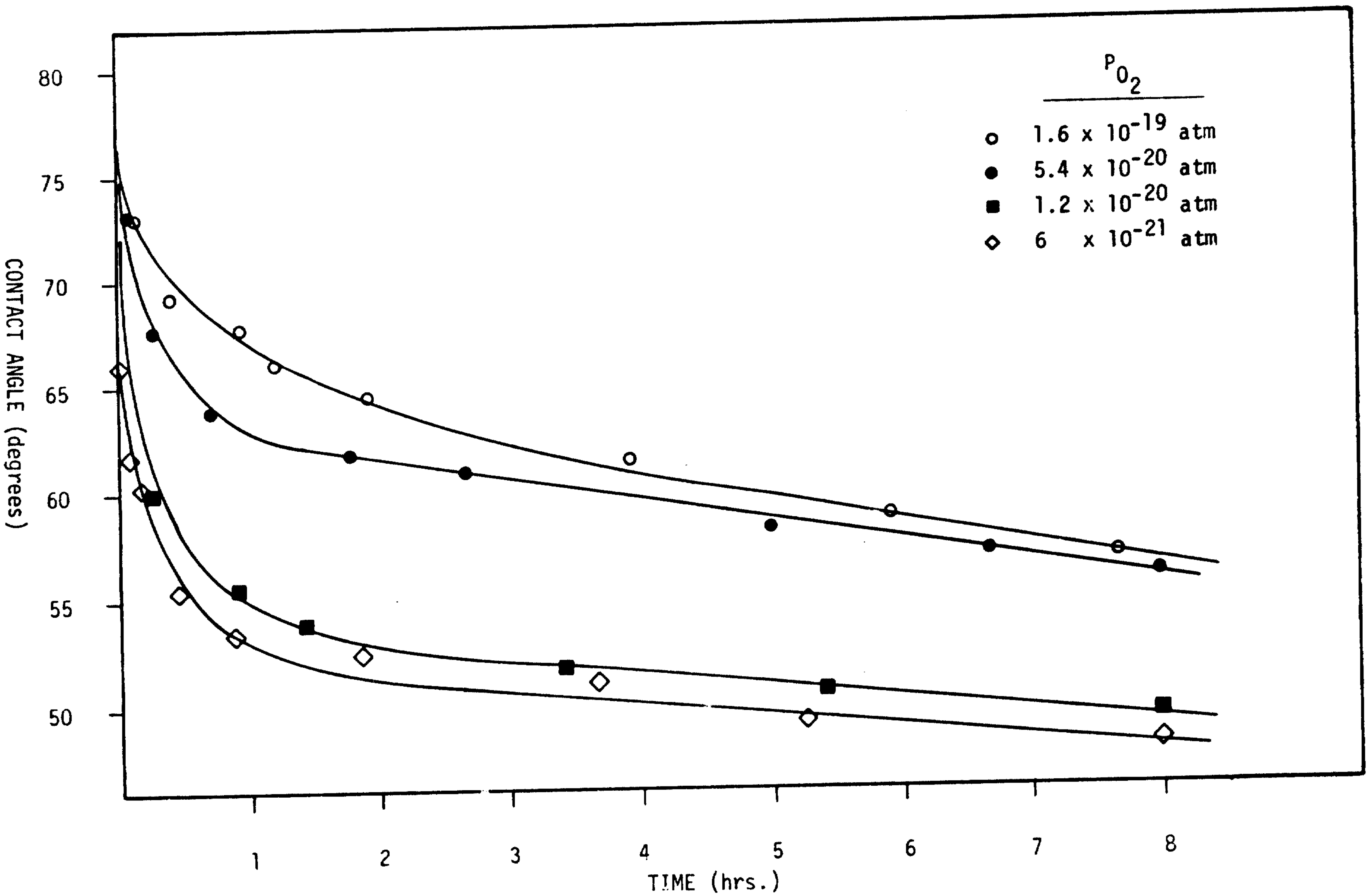

Figure 13. Molten Silicon Contact Angle on CNTD AlN as a Function of Time and P_{O_2}

2.4.3 Microscopic Examination of Sessile Drop Test Specimens

The interaction of molten silicon and CNTD coated SiC, Si_3N_4 and AlN, and the mode of molten silicon attack were explored by examination of polished cross sections of the silicon drop-CNTD coating interface of the post sessile drop test specimens. Two regions appeared for those specimens tested in the initial experiments: a heavily attacked region in the inner portion of the silicon drop, and a region of much reduced reaction situated at the outer portion of the drop. Optical photomicrographs (50X), focusing on the verge of the two regions in the Si - CNTD SiC interfaces after annealing at 1430°C in an oxygen partial pressure of 1.8×10^{-20} atm for: a) 2 hours, b) 8 hours, and c) 12 hours, are presented in Figure 14. The number and size of precipitates in the inner zone can be observed to increase as annealing time increases, while the outer zone remains apparently unattacked.

Since the degree of attack on the CNTD coatings was greater under the position of the original silicon cube (Figure 15, region A) than under the portion of the silicon drop which flowed away from the original cube position (Figure 15, region B), it suggested that there might be residual adsorbed oxygen between the silicon cube and the specimen which was not removed, being shielded from the flowing gas buffer. To check this possibility, a second configuration for the silicon cube was tried, called a "tilt configuration", where a small chip of silicon was placed under one edge of the silicon cube to provide a slight tilt as shown in Figure 16.

For the tilt configuration experiments on CNTD coated SiC, a sectioning scheme for the post sessile drop test specimens is shown in Figure 17 to show the position of the interface with respect to its original position before melting of the silicon cube. The appearance of these

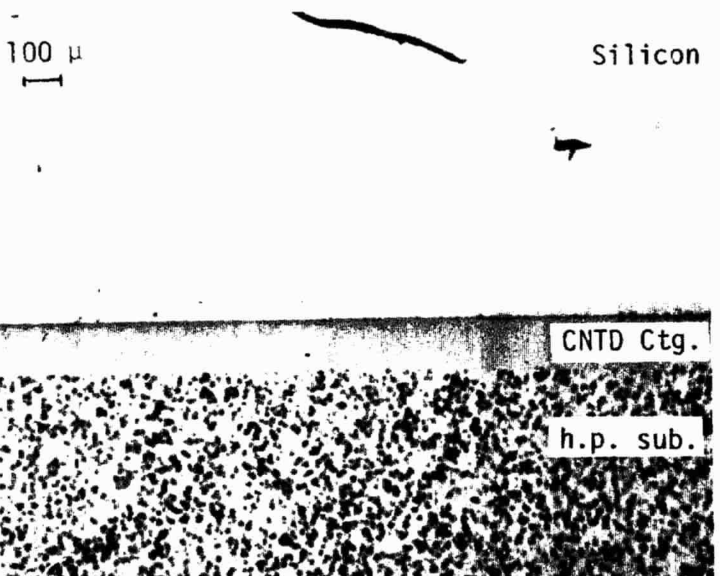

a) 2 hr

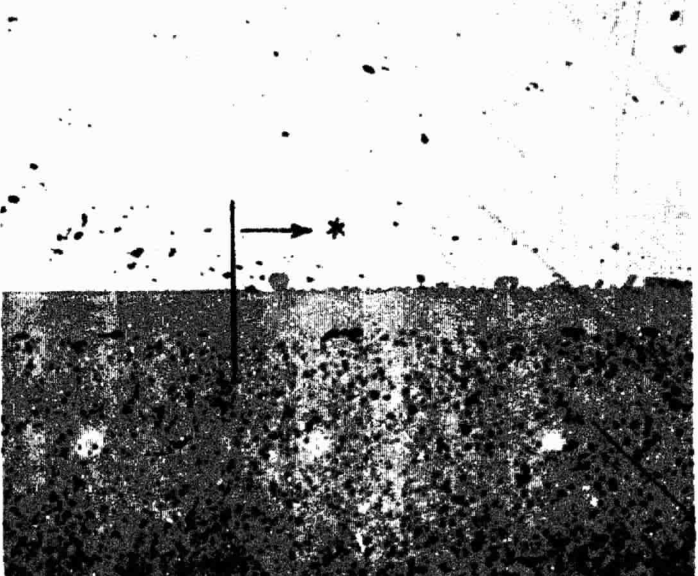

b) 8 hr

Figure 14. Interface Between Molten Silicon and CNTD SiC Annealed at $1430^{o}C$ and 1.8×10^{-20} atm P_{O_2}

Note greater reaction on inboard side (*) of verge between original position of cube and inert swept area (50X).

c) 12 hrs

Figure 14. (Cont.)

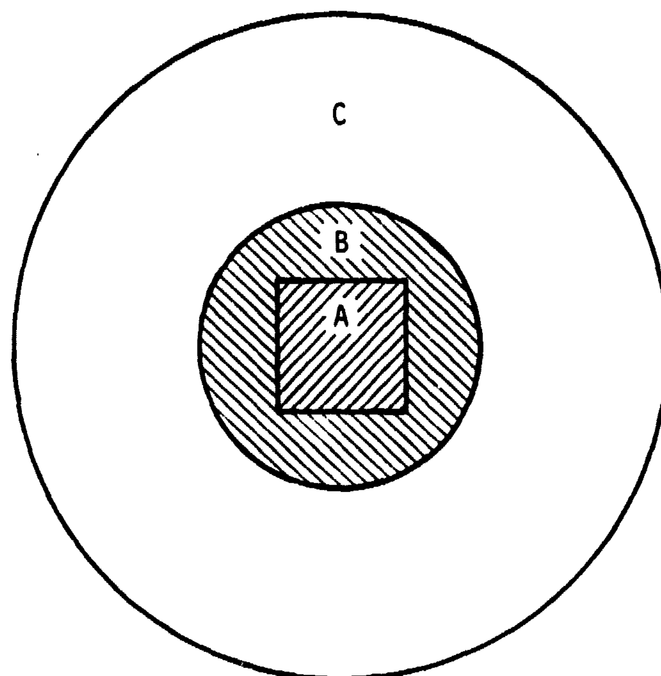

Region A - Position of Original Silicon Cube

Region B - Final Position of Silicon Drop

Region C - Specimen Not covered by Drop

Figure 15. Relative Positions of Original Silicon Cube, Silicon Sessile Drop, and Specimen

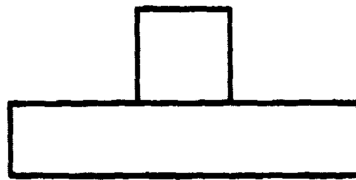

a) Normal Configuration

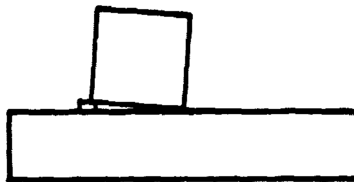

a) Tilt Configuration

Figure 16. Two Configurations for Silicon Cube Placement on Specimen

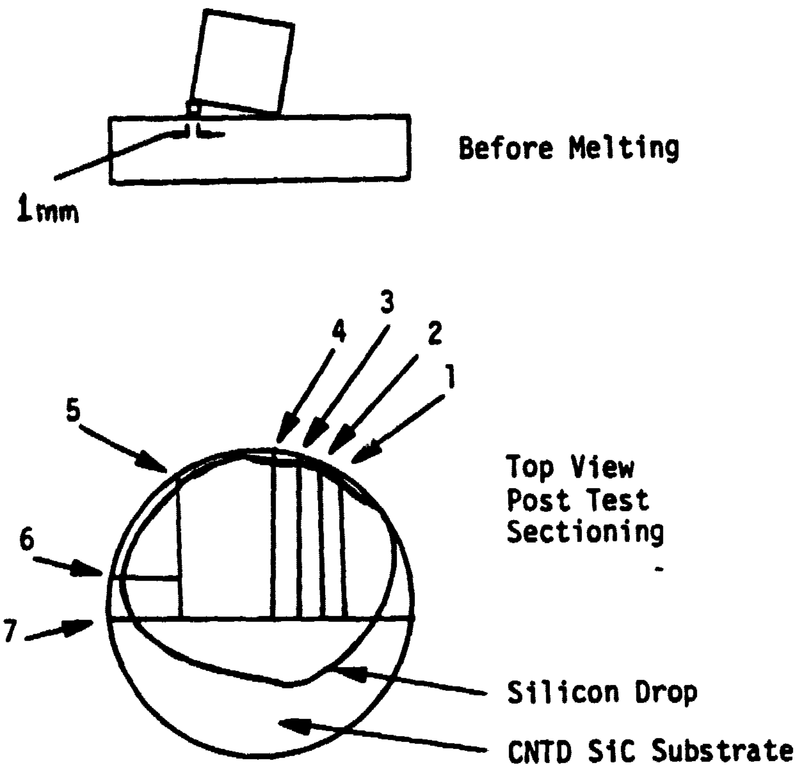

Figure 17. Slicing of Post Sessile Drop Specimen to Characterize Silicon - CNTD SiC Interface at Various Positions

specimens after this sectioning procedure is shown in Figure 18. It was observed on the 50X optical photomicrographs (Figure 19) that the only region with appreciable amounts of silicon attack was a short zone of about 1 mm length, corresponding to the size of the silicon chip used to tilt the silicon cube, while all other sections were essentially clear of any silicon attacked areas. Similar results were obtained for specimens tested using oxygen partial pressures of 2.3×10^{-19} atm., (Figure 20) substantiating the hypothesis of "trapping" adsorbed oxygen between the silicon cube and the substrate in the normal configuration experiments. Changes in the oxygen partial pressure in the range of 10^{-19} atm. to 10^{-20} atm. appear to have little effect on the degree of silicon attack on these CNTD coated specimens.

Examination of the unattacked regions of the Si-CNTD coating interface by the employment of SEM reveals that there is still negligible interaction observable even at a magnification of 1750X. An SEM micrograph of such an interface after a sessile drop test is shown in Figure 21.

Above the Si-SiO_2 equilibrium P_{O_2} the molten silicon attacking mode appears to proceed by a process of dissolution and precipitation of the coating material, where oxygen acts as a catalyst to lower the activation energy for the dissolution of the coating material.

A tilt configuration silicon - CNTD coated Si_3N_4 experiment was tried to establish whether silicon attack would be reduced as in the SiC experiments. Figure 22, showing the interface of such a post sessile drop experiment specimen, exhibits the expected reduction of attack.

For comparison purposes, one series of experiments was conducted on hot pressed Si_3N_4 without a CNTD coating. Figure 23 shows optical

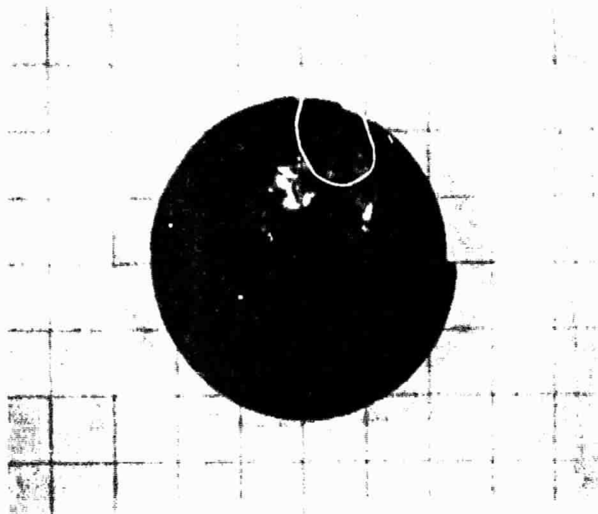

a) $P_{O_2} = 2.3 \times 10^{-19}$ atm

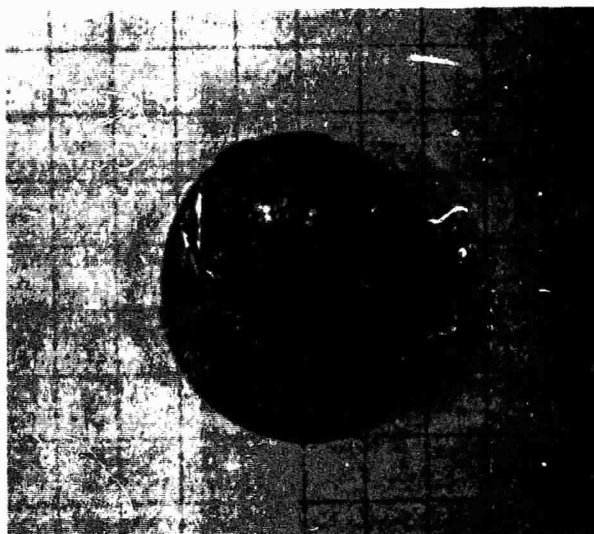

b) $P_{O_2} = 2.6 \times 10^{-20}$ atm

Figure 18. Post Sessile Drop Test Specimens of CNID SiC
Tilt Configuration, 1430°C, for differing P_{O_2}

Silicon

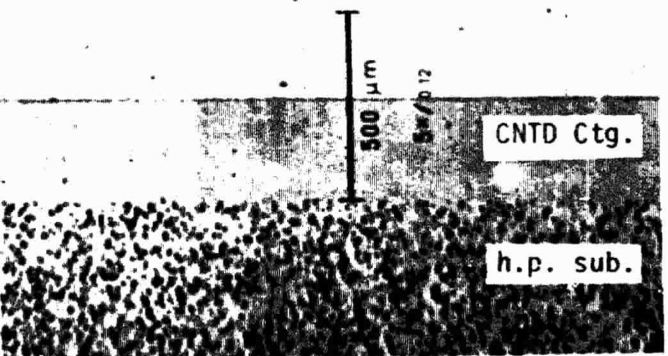

a) Typical Section

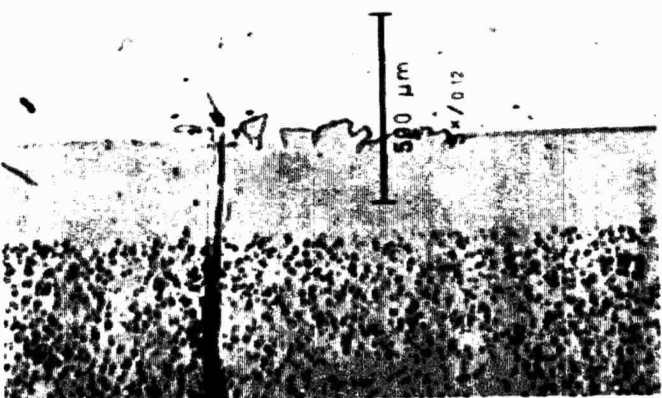

b) Section 5
(ref. fig. 17)

Figure 19. Molten Silicon - CNTD SiC Interface
to Investigate Effects of Tilt Configuration

Note reaction observed at position corresponding
to the "prop chip" position in tilt configuration. (50X)

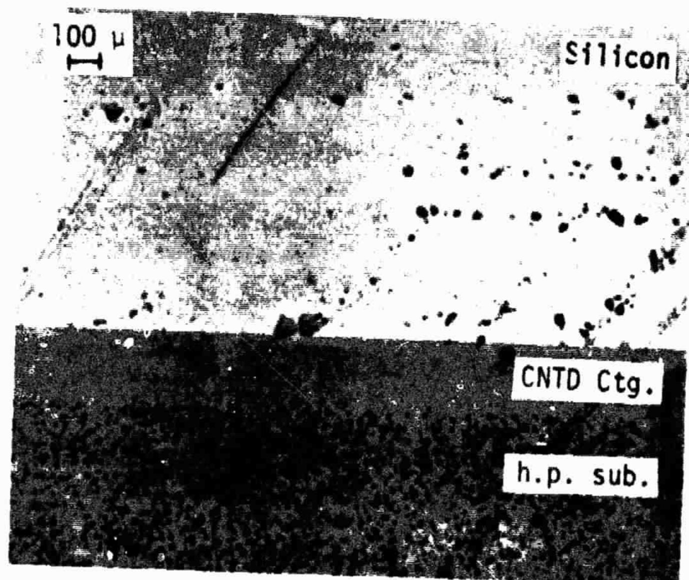

Figure 20. Singular Reaction Point for Tilt Configuration Experiment on CNTD SiC

50X, 8 hrs, 1430°C, 2.3 x 10^{-19} atm P_{O_2}

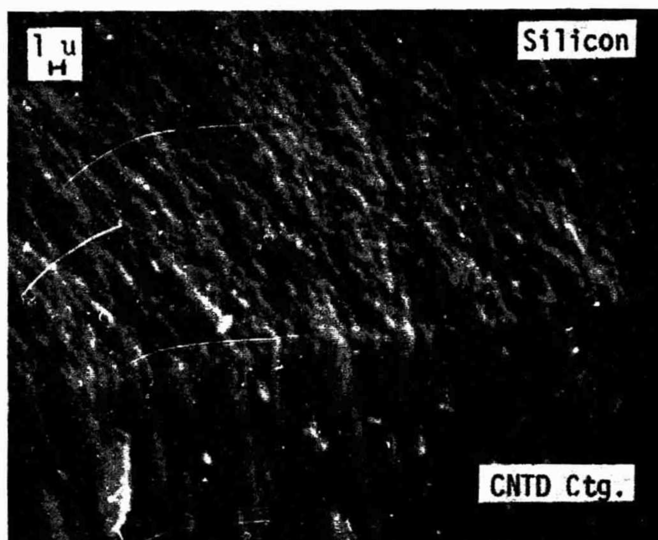

1750X

Figure 21. Typical Scanning Electron Micrograph of Molten Silicon - CNTD SiC Interface

From a clean interface region such as that observed in Figures 19 and 20.

100X

Figure 22. Molten Silicon - CNTD Si_3N_4 Interface, Tilt Configuration

8 hrs., 1430°C, 1.6×10^{-19} atm P_{O_2}

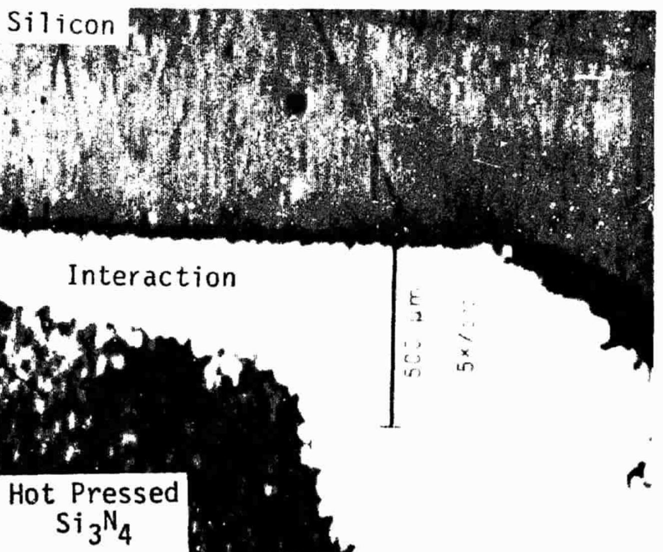

a)

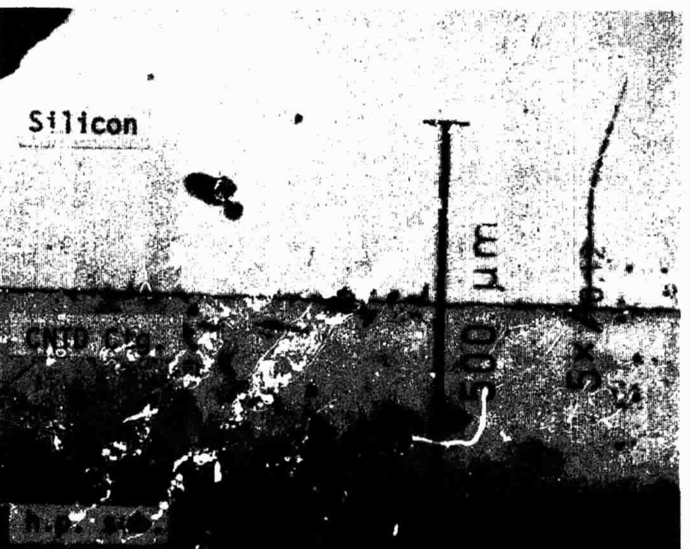

b)

Figure 23. Comparison of Degree of Molten Silicon Attack of Hot Pressed and CNTD Si_3N_4

12 hrs, 1430°C, 1.8×10^{-20} atm P_{O_2}

a) Hot pressed (50X)
b) CNTD (100 X)

photomicrographs of silicon-specimen interfaces for a CNTD coated Si_3N_4 sample and a hot pressed Si_3N_4 sample. After sessile drop testing, much less silicon penetration occurred in the sample having the CNTD coating than in the hot pressed sample, indicating the importance of the surface properties provided by the CNTD process, which obviously can greatly improve the capacity of these materials to withstand attack by molten silicon.

2.4.4 Auger Analysis

Oxygen contamination on as-received CNTD coated polished samples was checked through AES analysis on a specimen prior to the sessile drop test. The results (Figure 24) indicate that a large amount of oxygen contamination exists on the surface of these specimens, in further agreement with the foregoing observations regarding oxygen trapping under the silicon cube. Reduction of this adsorbed oxygen by placing the CNTD coated samples in a low P_{O_2} ambient atmosphere prior to the covering of the substrate by molten silicon should significantly reduce the degree of silicon attack on these materials.

Surface analysis by AES was possible for investigating the interaction of CNTD coated AlN with silicon because the major constituent species in the AlN does not contain silicon as it did in the case of SiC and Si_3N_4. AES analysis of the CNTD AlN surface prior to a sessile drop test is presented in Figure 25, revealing that oxygen and carbon are the primary contaminants on the surface. The surface of CNTD coated AlN outside the silicon drop, after a 1-hour sessile drop test, was covered by a thin layer of silicon (Figure 26-a). A ten-minute sputtering removes all the silicon signal and shows exactly the same AES spectrum as the surface analysis of the pre-sessile drop specimen. (Figure 26-b)

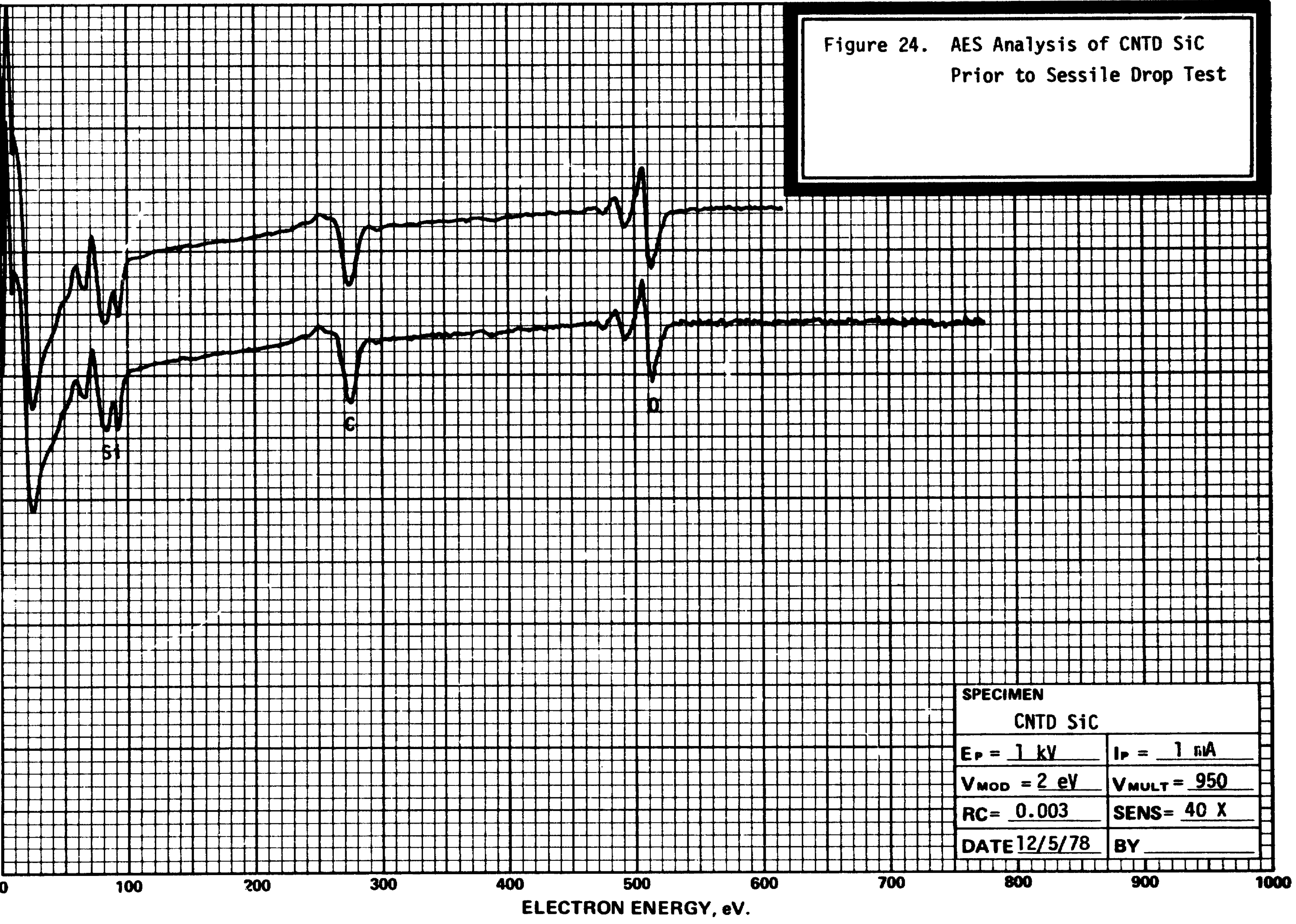

Figure 24. AES Analysis of CNTD SiC Prior to Sessile Drop Test

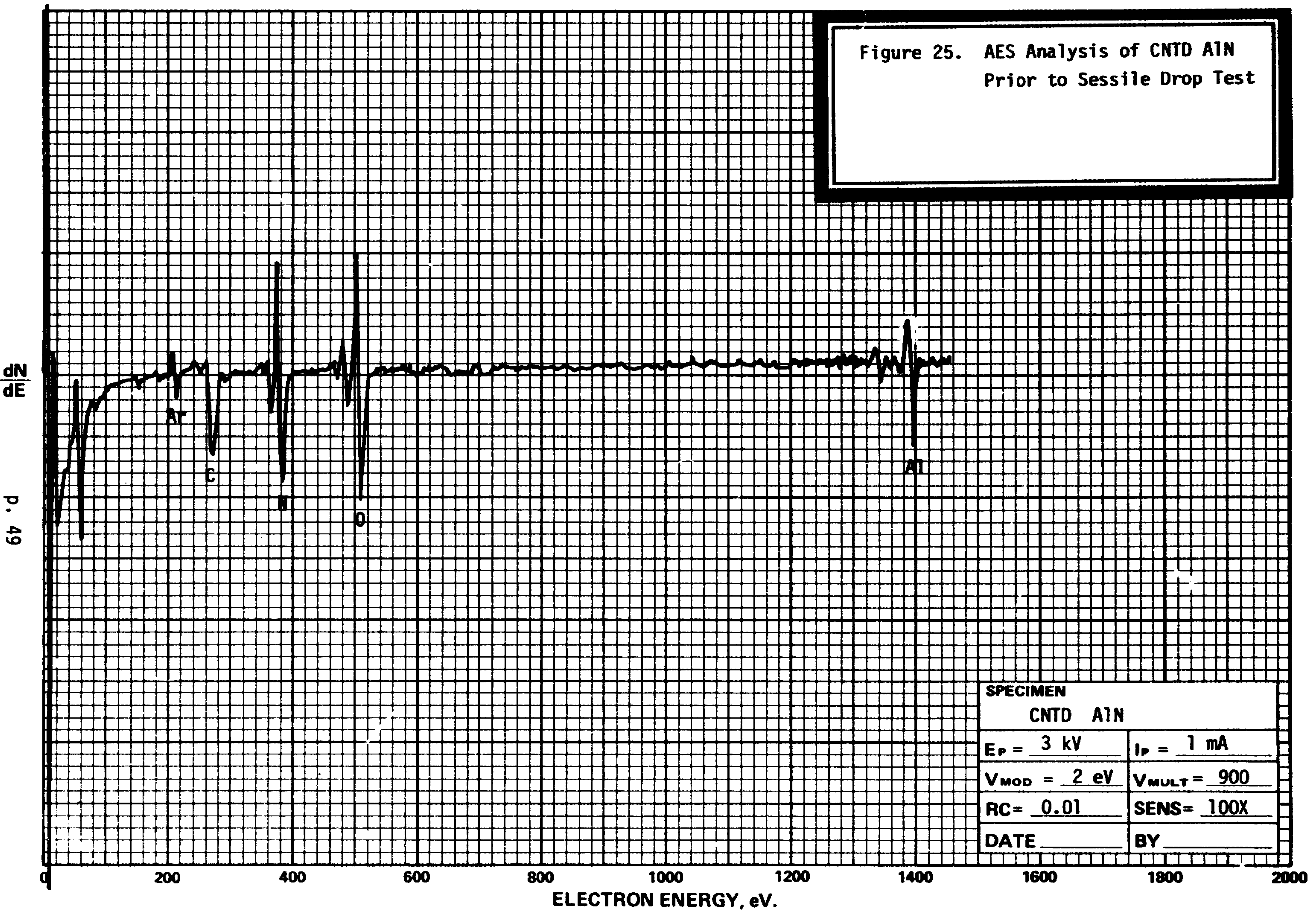

Figure 25. AES Analysis of CNTD AlN Prior to Sessile Drop Test

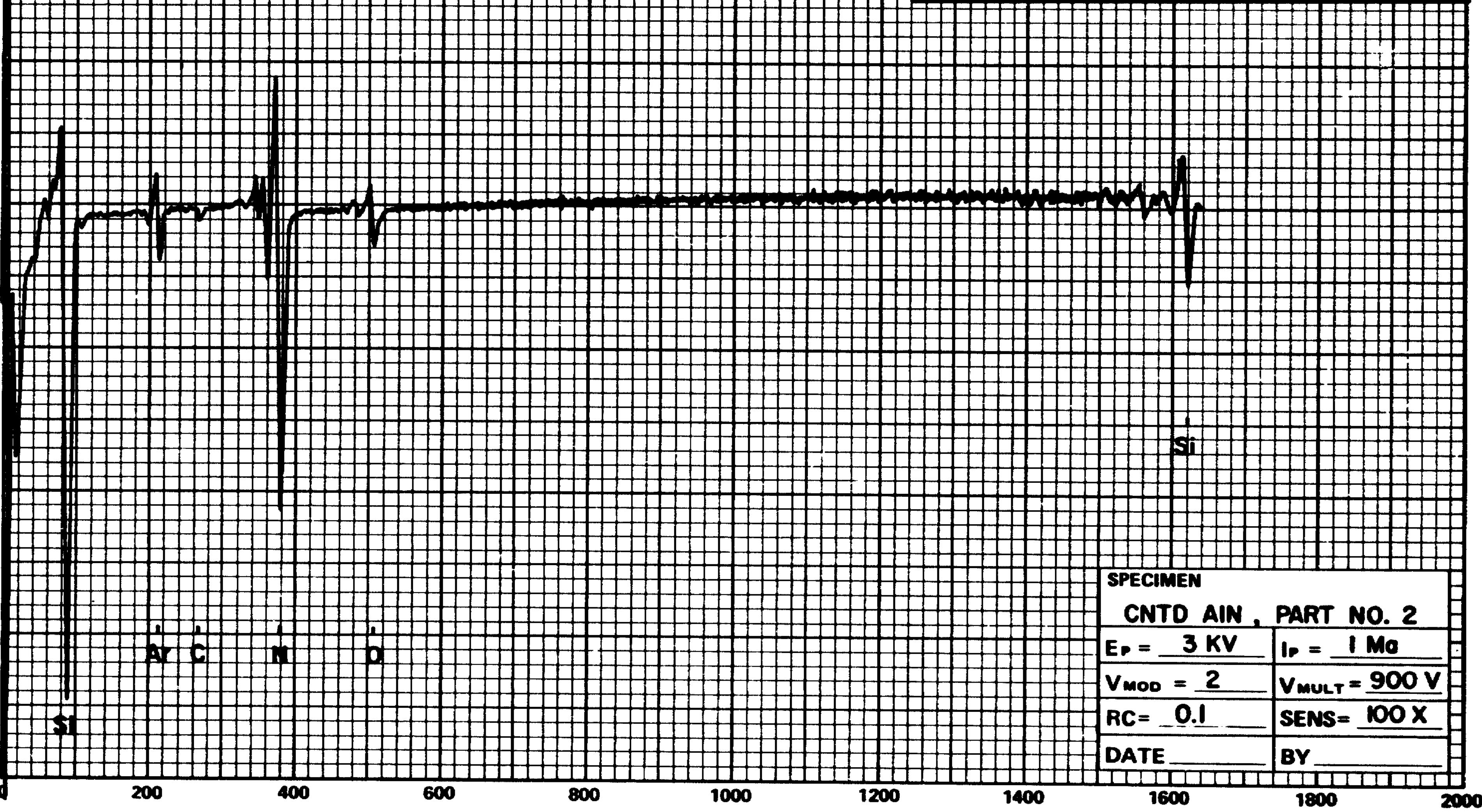

Figure 26-a. Post Sessile Drop Auger Electron Surface Analysis, CNTD AlN

After 2 min. sputtering

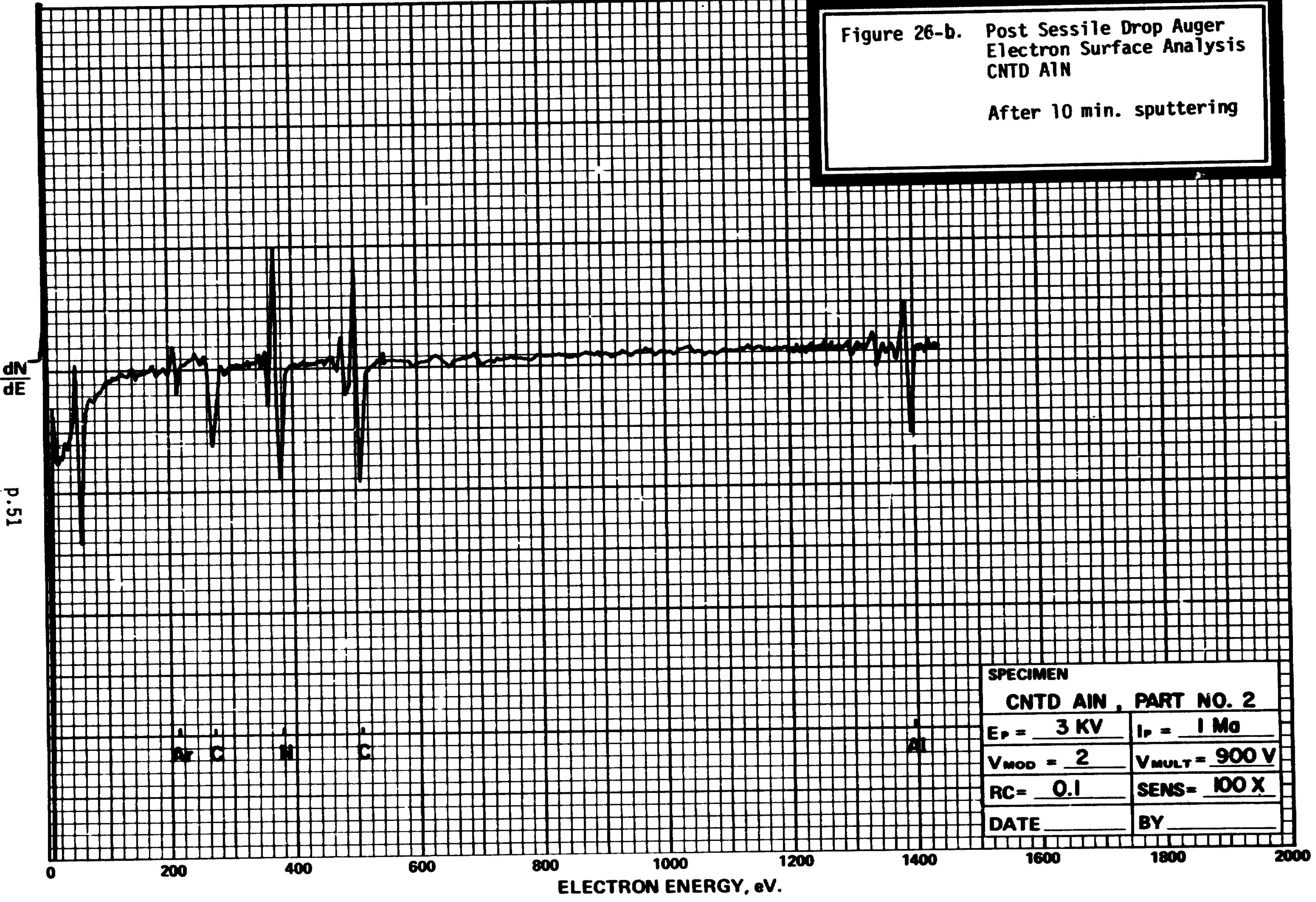

Figure 26-b. Post Sessile Drop Auger Electron Surface Analysis CNTD AlN

After 10 min. sputtering

Figures 27-a, b, and c, show AES analysis near the bottom of the silicon drop. To obtain the analysis the silicon drop was cut away from the AlN substrate leaving a thin layer of silicon which was etched and polished. In a region near the center of the drop (Figure 15, region A) the nitrogen content inside the silicon layer is found to be very high suggesting that the AlN was dissolved in the silicon. At another location, near the outer portion (Figure 15, region B) of the silicon drop, (Figures 28 - a and b) the nitrogen signal is not present until after 17.5 minutes of sputtering, at which time the silicon signal disappears and the spectrum becomes the same as for AlN prior to sessile drop testing, indicating a sharp silicon - AlN interface. This supports the conclusion that the adsorbed oxygen under the silicon cube enhances the interaction between the molten silicon and the AlN substrate by promoting dissolution of the substrate and subsequent precipitation in the silicon.

2.4.5 Separation of CNTD Coatings From Substrates

The interface between the CNTD coatings and the hot pressed substrates remains essentially unchanged after sessile drop experiments at 1430^{0}C for 8 hours, as shown in Figure 29. Occasional separation of the coating layer from the substrate after sectioning a post-sessile drop test specimen, however, is observed (Figures 30 and 31).

An examination of the reverse side of the mechanically separated CNTD coatings by SEM, (Figure 32 and 33) reveals no evidence of the presence of free silicon. No such evidence of free silicon penetration of the CNTD coatings was ever observed in our experiments. Thus, the separation of the CNTD coatings from the hot pressed substrates appears to be the result of mechanical failure in the bond during the cutting process rather than the action of silicon attack.

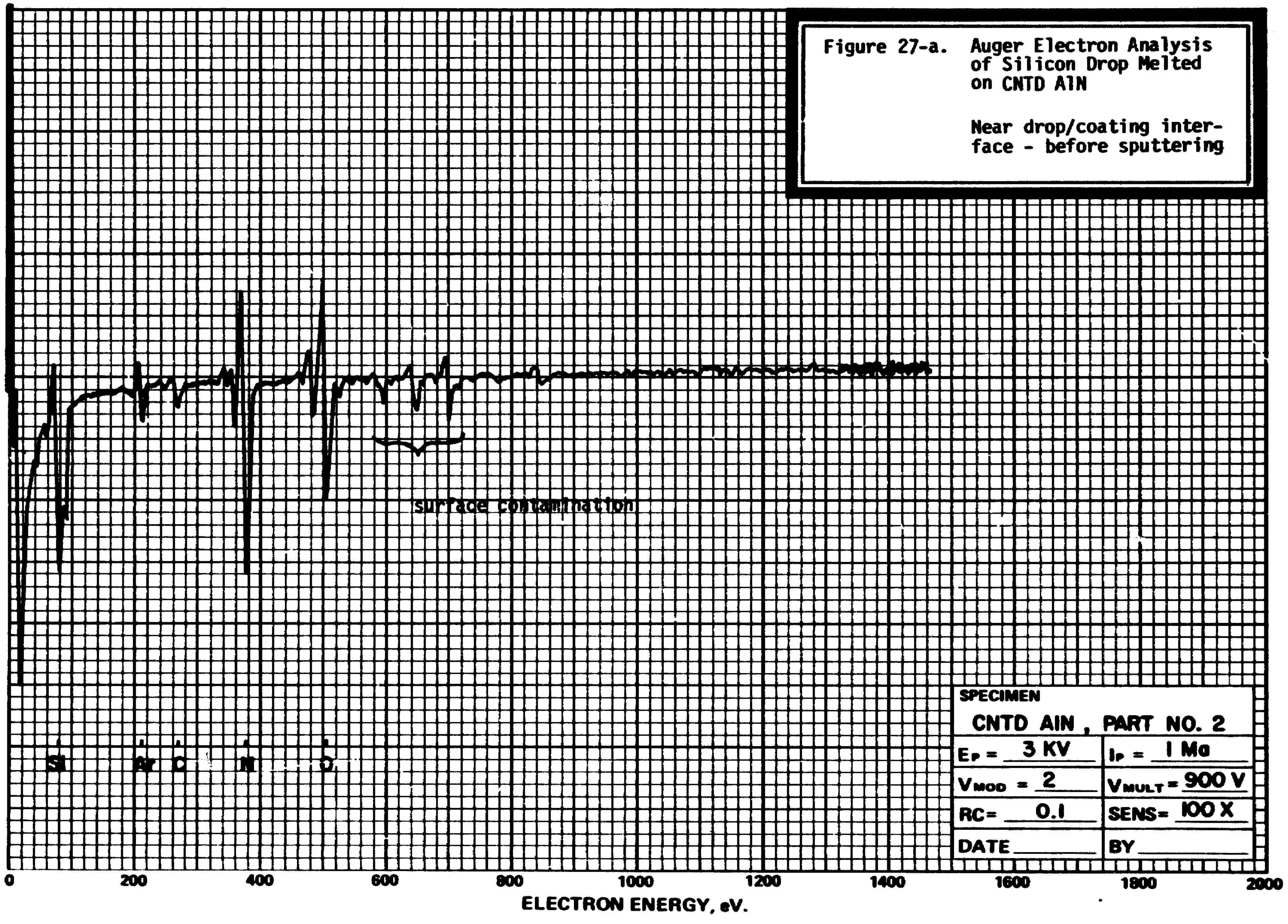

Figure 27-a. Auger Electron Analysis of Silicon Drop Melted on CNTD AlN

Near drop/coating interface - before sputtering

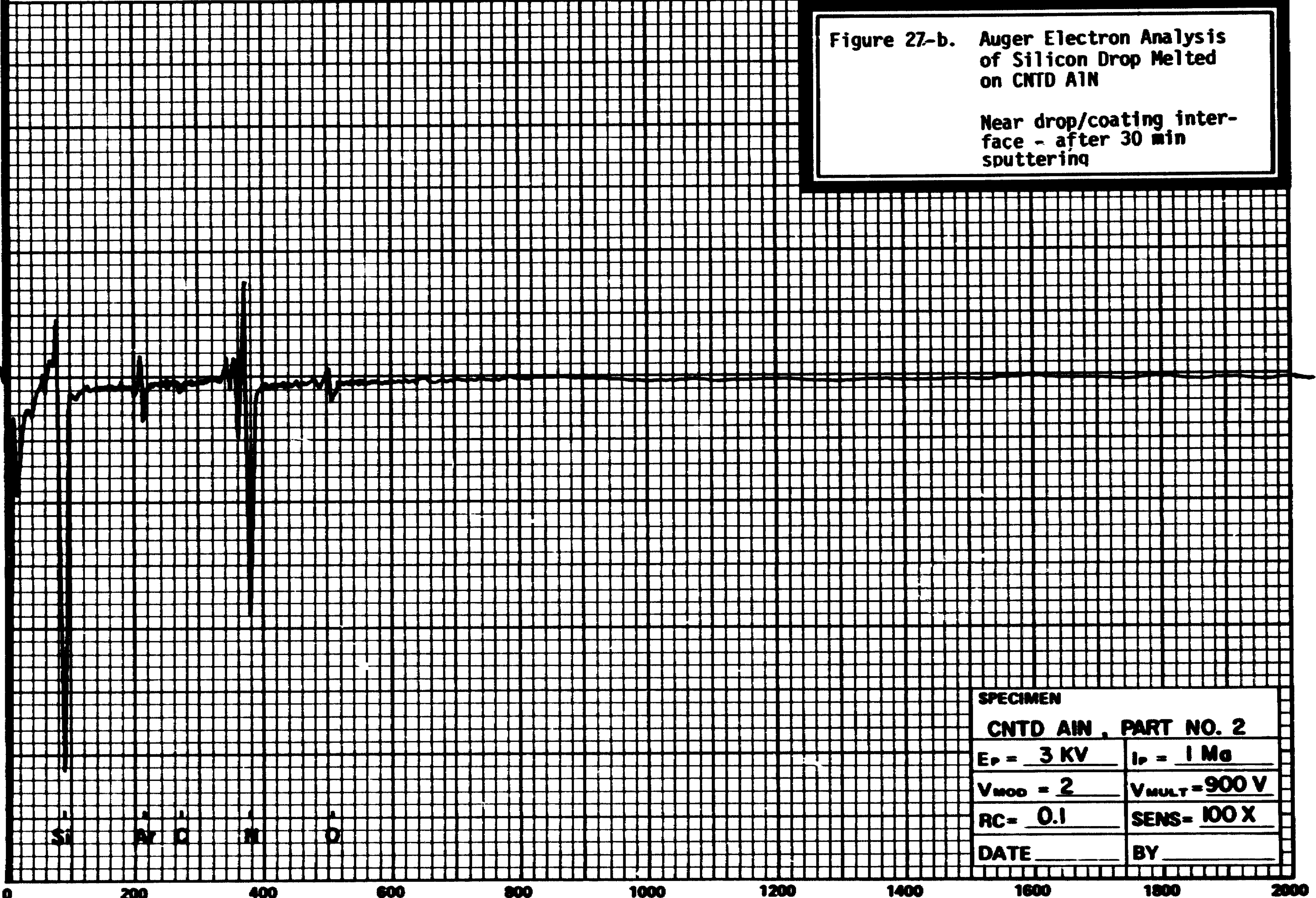

Figure 27-b. Auger Electron Analysis of Silicon Drop Melted on CNTD AlN

Near drop/coating interface - after 30 min sputtering

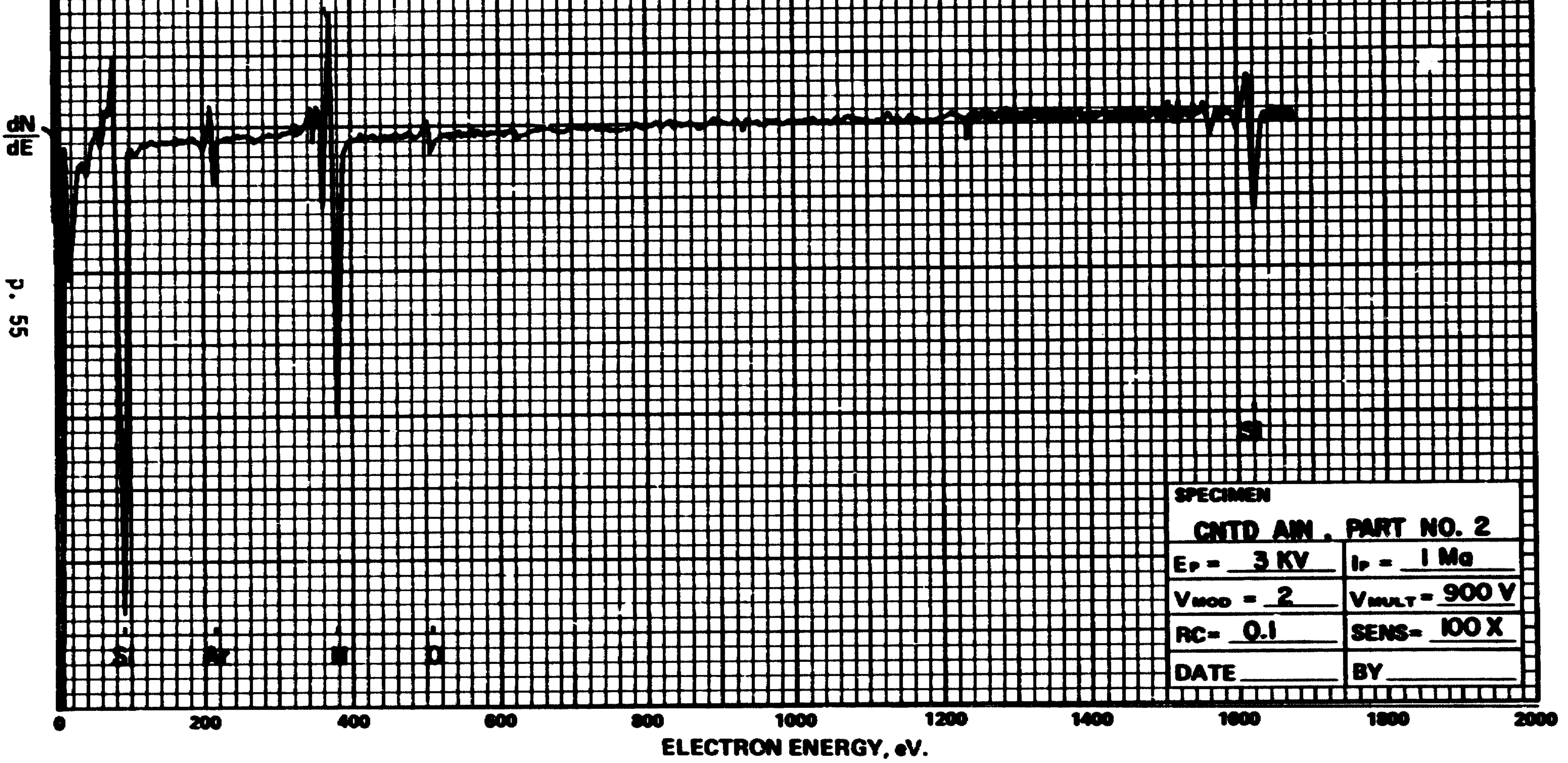
Figure 27-c. Auger Electron Analysis of Silicon Drop Melted on CNTD AlN
Near drop/coating interface - after 87 min. sputtering
dN/dE
Si
O
Si
SPECIMEN
CNTD AlN , PART NO. 2
EP = 3 KV
IP = 1 Ma
VMOD = 2
VMULT = 900 V
RC= 0.1
SENS= 100 X
DATE
BY
0
200
400
600
800
1000
1200
1400
1600
1800
2000
ELECTRON ENERGY, eV.

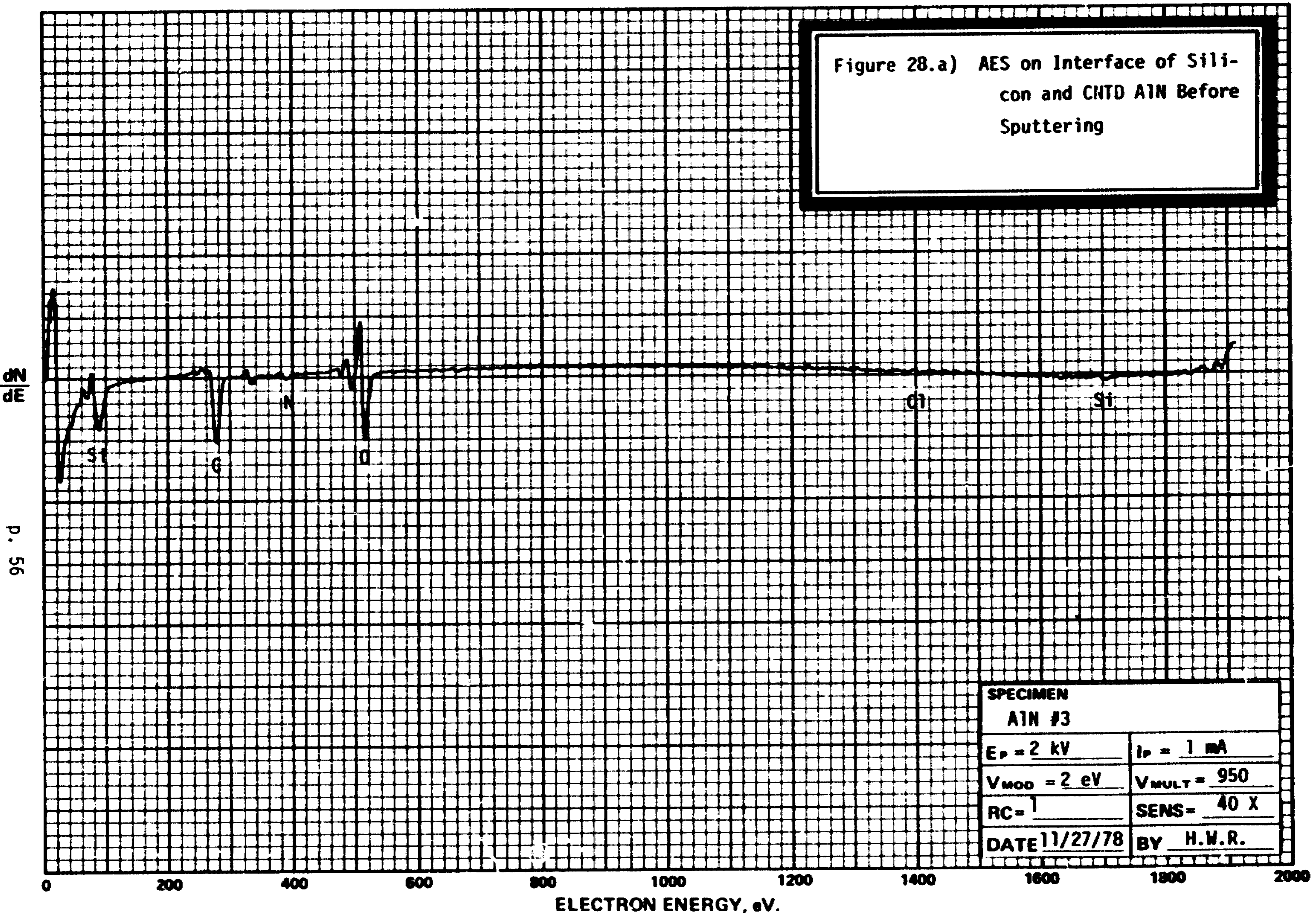

Figure 28.a) AES on Interface of Silicon and CNTD AlN Before Sputtering

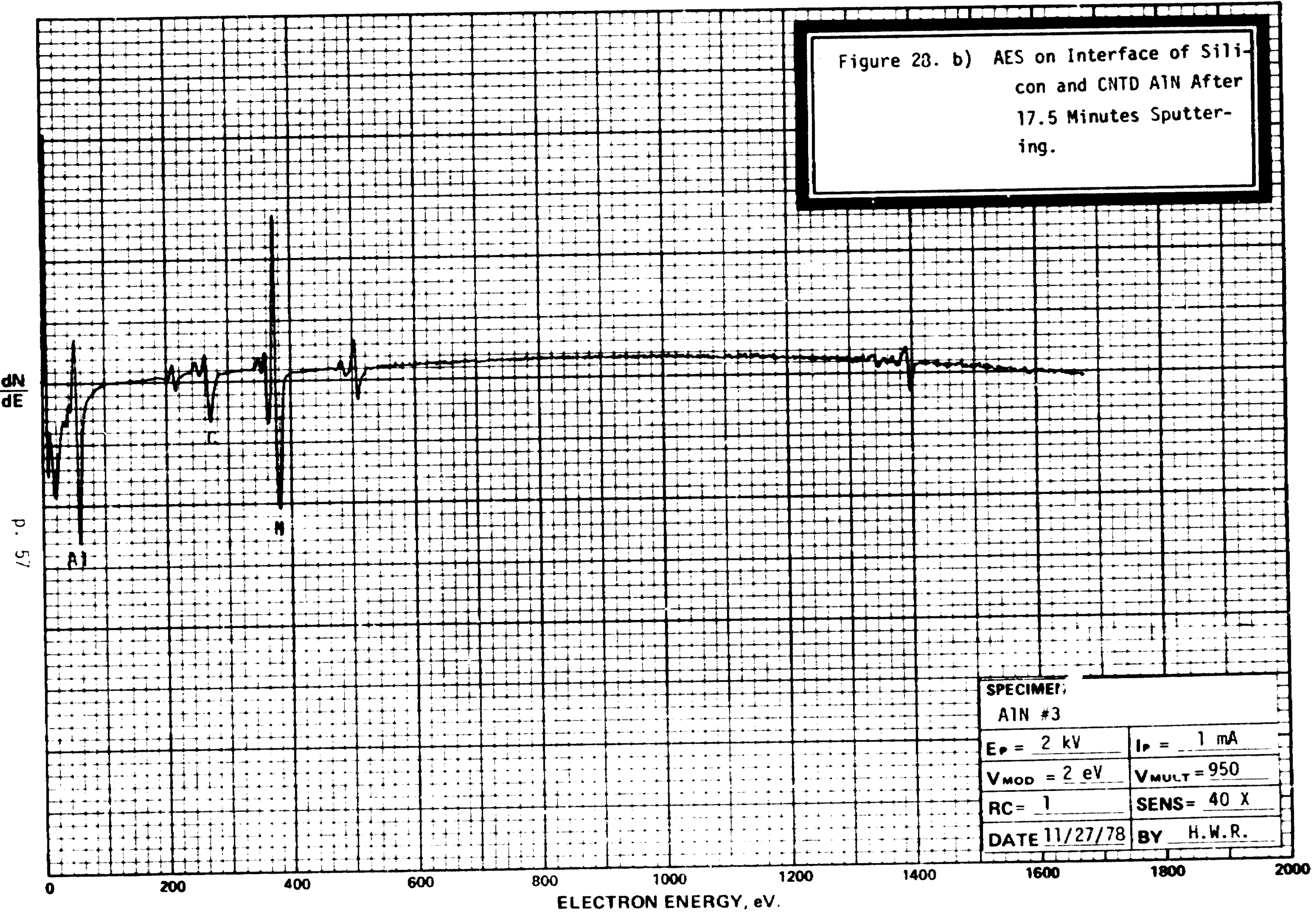

Figure 28. b) AES on Interface of Silicon and CNTD AlN After 17.5 Minutes Sputtering.

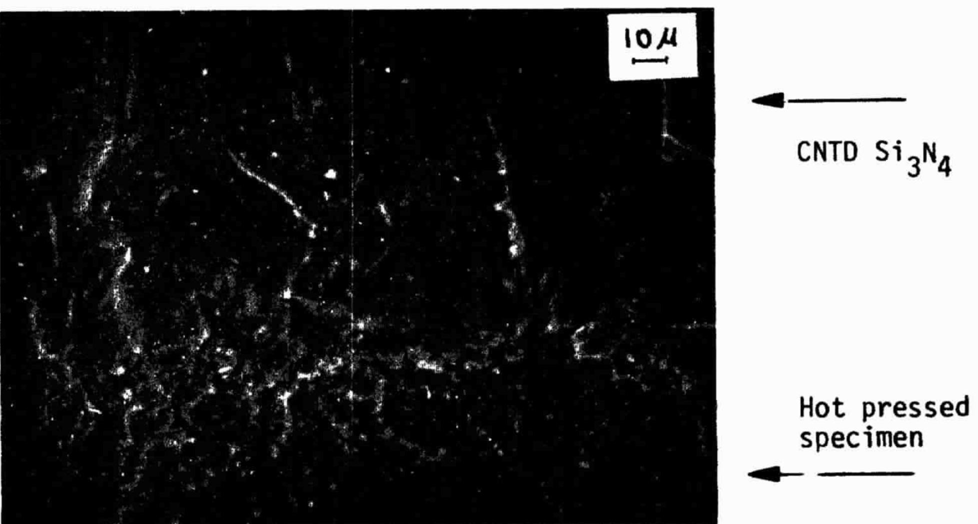

Figure 29. Scanning Electron Photomicrograph of CNTD Si_3N_4 - Hot Pressed Specimen Interface After Sessile Drop Testing

500X, 8 hrs., 1430°C

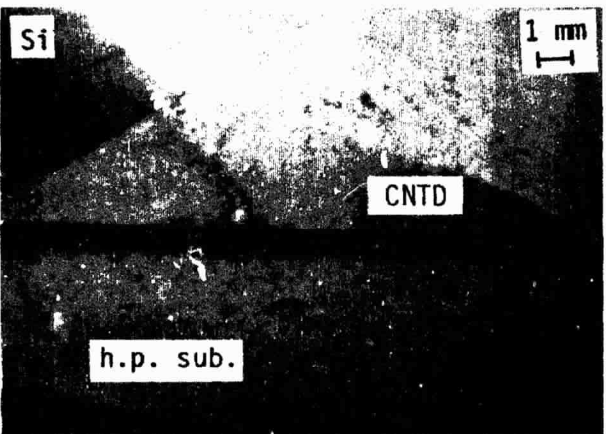

Figure 30. Separation of CNTD Si_3N_4 Coating From Hot Pressed Substrate

Separation occurred during sectioning, 5X

Figure 31. Separation of CNTD SiC Coating from Hot Pressed Substrate

Separation occurred during sectioning.

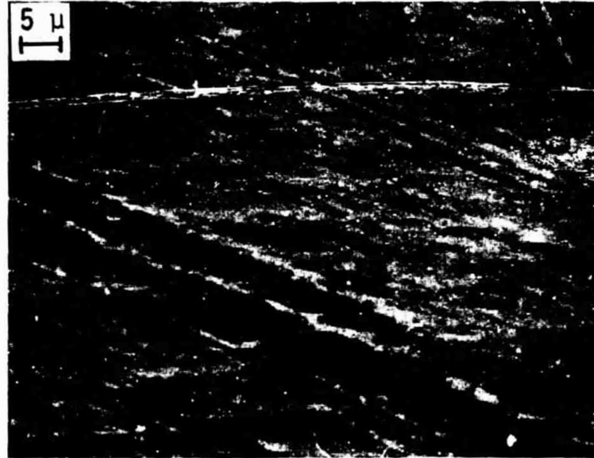

Figure 32. Scanning Electron Photomicrograph of Reverse Side of a Separated CNTD Si_3N_4 Coating

1200X, no evidence of molten silicon

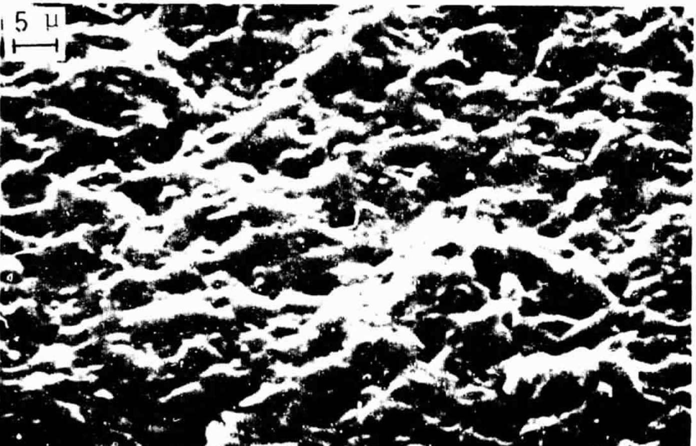

a)

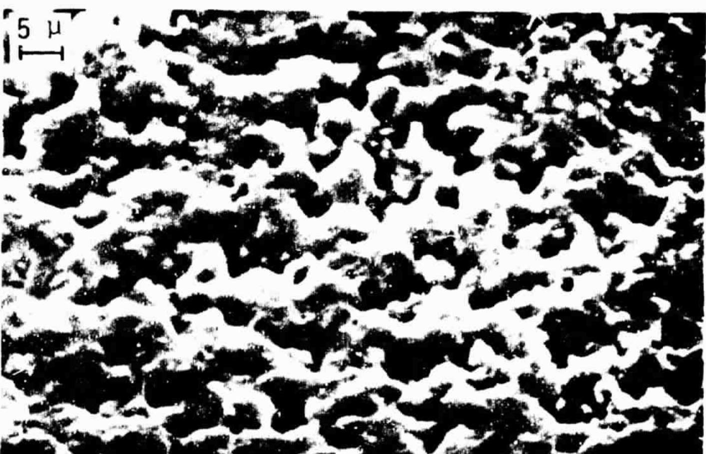

b)

Figure 33. Scanning Electron Photomicrograph of the Reverse Side of a Separated CNTD SiC Coating

No evidence of molten silicon penetration, 1200X.

a) Directly under silicon drop
b) Away from silicon drop area

2.4.6 Conclusions

A) Of the samples tested, CNTD coated SiC appears to have the highest resistance to molten silicon attack.

B) Of the three CNTD coatings tested, SiC is most wetted, exhibits the greatest stability of contact angle with time and is the most sensitive to changes in oxygen partial pressure in the range investigated.

C) The contact angle of molten silicon measured on the samples as a function of time at a fixed P_{O_2} decreased, more rapidly at first, tending toward a constant small rate of change after 1 hour.

D) Increasing the oxygen partial pressure increases the contact angle, apparently because adsorbed oxygen lowers the solid-vapor interfacial free energy.

E) Adsorbed oxygen increases the degree of attack of molten silicon on CNTD coated SiC, Si_3N_4, and AlN. The effect is minimized by allowing the solid surfaces to equilibrate with the low P_{O_2} environment prior to melting.

F) The fine grained, dense CNTD coatings greatly reduce the amount of molten silicon attack compared to uncoated hot pressed samples of the same nominal chemical composition.

2.5 MANUFACTURING OF CONTAINERS AND DIES

Test specimens representative of the four candidate materials systems were characterized at MRL as described in section 2.3 and evaluated for stability in contact with liquid silicon under atmospheres of varying oxygen partial pressure at UMR as described in section 2.4. The Program Organization (Figure 1) called for the selection of materials systems for hardware delivery, ie. containers and dies, based upon the preceding evaluations.

The systems chosen for container and die fabrication and delivery were CMS-1, SiC, and CMS-2A, Si_3N_4. CMS-2A was chosen over 2B because of the lower raw material cost and greater fabricability associated with the lower purity Si_3N_4 powder. The CMS-1 and CMS-2 materials showed a great deal of promise in the sessile drop testing at UMR. The CMS-3, AlN, was not carried over to container and die fabrication because of its greater susceptibility to attack by molten silicon. CMS-4 materials, altered Si_3N_4, were found to be much like the CMS-2 materials, with x-ray diffraction showing the CNTD coatings to be α-Si_3N_4 in both cases. The CMS-2 materials were chosen over the CMS-4 materials because of the greater consistency observed for CMS-2 attributes (crystallite size and diffraction patterns) among specimens.

2.5.1 Fabrication of Containers

The containers for CNTD coating application were fabricated by hot pressing the powders in graphite molds. The powder preparation was the same as for the specimen discs. These preparation procedures and the hot pressing conditions are given in the Process Specifications in the Appendices.

The first articles of the full size container shape were simple right circular cylinders with a slightly tapered inner wall surface and

a rounded bottom inside. The outside bottom was flat and perpendicular to the outside walls. The dimensions were 2-1/2" O.D. x 2" I.D. x 1-1/2" deep x 1-3/4" overall height. Containers of this geometry were plagued by a tendency to exhibit circumferential voids and cracks where the inside wall blended into the rounded bottom. Various techniques of charging the powder to the tooling were attempted, and these were only partially successful in alleviating the problem.

The phenomenon seemed to be related to the powder flow problems inherent in forming a part with a thin walled section on a relatively massive base. This was solved by machining a recess in the punch which formed the containers outside bottom thereby changing the shape from that of a right circular cylinder to the frustum of a cone with a 60° angle of divergence at the projected tip. The cone was truncated such that a stable base was provided for the container. The tooling modification described above was designed to increase the pressure component perpendicular to the inner wall at the point of blending into the rounded bottom. The final container design is shown in Figure 34. After adopting these design changes containers of 85.5 to 86% theoretical density were fabricated in SiC (w/1 wt% B) and of 90.3 to 92.8% theoretical density in Si_3N_4 (w/4 wt% MgO), and the circumferential voids and cracks were eliminated.

The hot pressed containers were coated on all surfaces (inner and outer) with the compatible CNTD coating. The containers were not ground prior to coating in order to provide parts prototypic of a reasonable production process. The as-pressed surface condition was reasonably smooth and the CNTD coatings covered the existing surface irregularities without interruption. Photographs of the CNTD coated containers, as delivered, are shown in Figure 35.

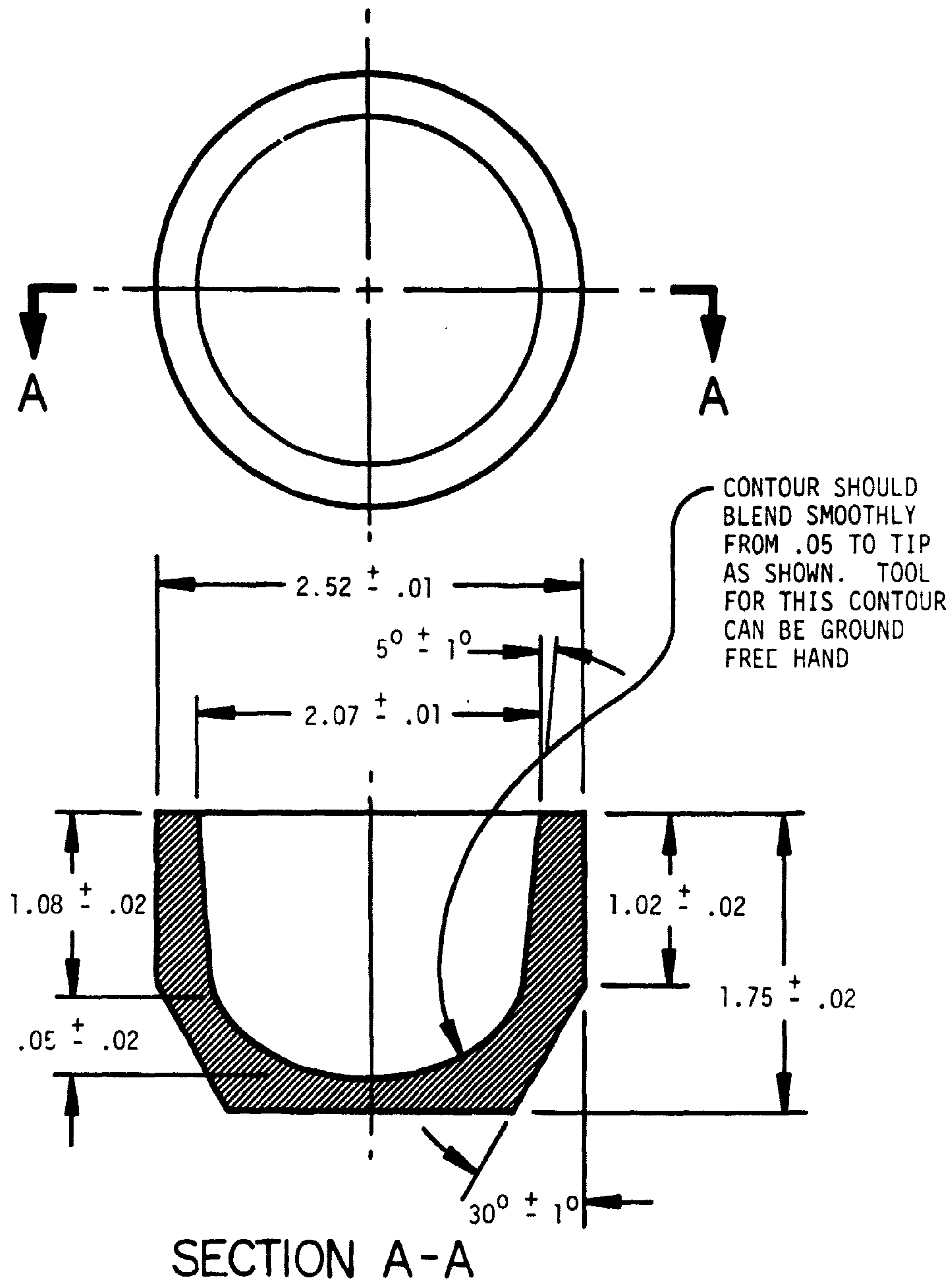

Figure 34. Hot Pressed Ceramic Container Design

a)

b)

Figure 35. CNTD Coated Containers, as Delivered

a) CNTD SiC on hot pressed SiC (1 wt% B)

b) CNTD Si_3N_4 on hot pressed Si_3N_4 (4 wt% MgO)

The CNTD Si_3N_4 container coatings were essentially transparent, approximately 0.005" thick, and uniform in appearance across the surface. X-ray diffraction showed the coatings to be crystalline α-Si_3N_4. The crystalline morphology is illustrated in the photomicrograph of the as-deposited coating, Figure 36.

The CNTD SiC container coatings were 0.005" thick and were shown by x-ray diffraction to be crystalline β-SiC. The surface reflectance varied somewhat across the surface as a function of smoothness, but the as-deposited surface was, in general, essentially the same as that shown in Figure 2.

2.5.2 Fabrication of Dies

The same candidate materials systems (CMS - 1 and 2) that were selected for container hardware delivery were also chosen for die delivery requirements. Die blanks were hot pressed in graphite tooling from SiC w/1 wt% B and Si_3N_4 w/4 wt% MgO. The as-pressed blanks were rectangular slabs, 1.30" x 1.15" x the appropriate thickness. Average densities of the hot pressed blanks were 90.1% theoretical density for SiC (w/1 wt% B) and 95.9% theoretical for Si_3N_4 (w/4 wt% MgO).

The hot pressed blanks were machined, by sawing or grinding with fixed diamond abrasive, to the required geometry. During the course of this program ceramic dies of both one and two-piece designs were machined for subsequent CNTD coating application. The original one and two-piece die designs suggested by the Jet Propulsion Laboratory are shown in Figures 37 and 38 respectively. These designs were developed for fabrication from graphite which can be machined with less applied stress than brittle ceramics. Graphite is also amenable to low cost machining operations such as milling, while ceramics are not.

Figure 36. Scanning Electron Photomicrograph of CNTD Si_3N_4 Coating, CMS-2 Container. 1500X, as deposited.

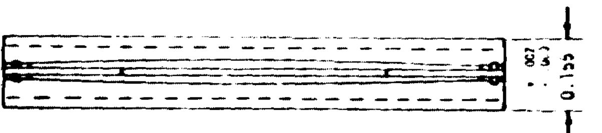

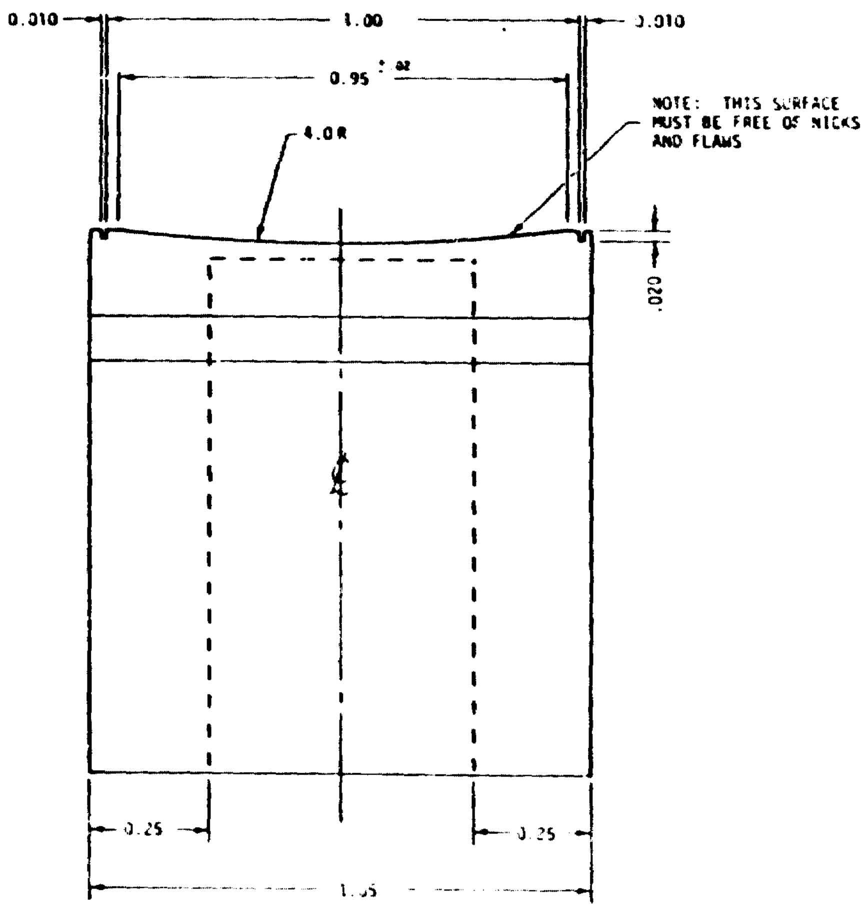

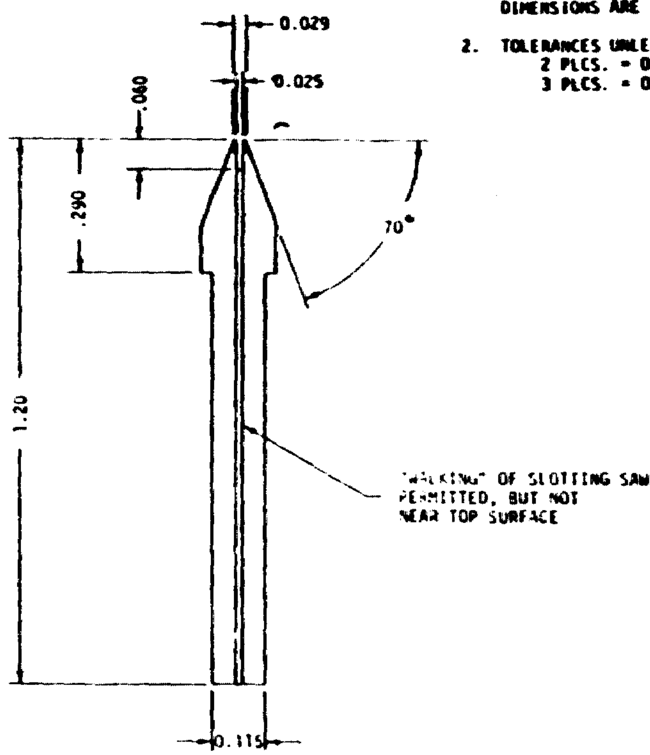

EAGLE-PICHER INDUSTRIES, INC. SPECIALTY MATERIALS DIVISION			
ONE PIECE DIE			
SCALE APPROXIMATELY 4" = 1"		DATE	8 SEPT 78
DRAWN JMF			
	DRAWING NO.	EXHIBIT 1 TO CONTRACT NO. 954877	

NOTES:
1. UNLESS OTHERWISE NOTED ALL DIMENSIONS ARE IN INCHES
2. TOLERANCES UNLESS OTHERWISE NOTED:
   2 PLCS. = 0.01
   3 PLCS. = 0.003

Figure 37. JPL Suggested One Piece Die Design

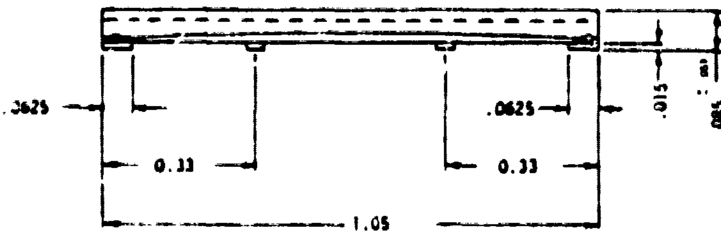

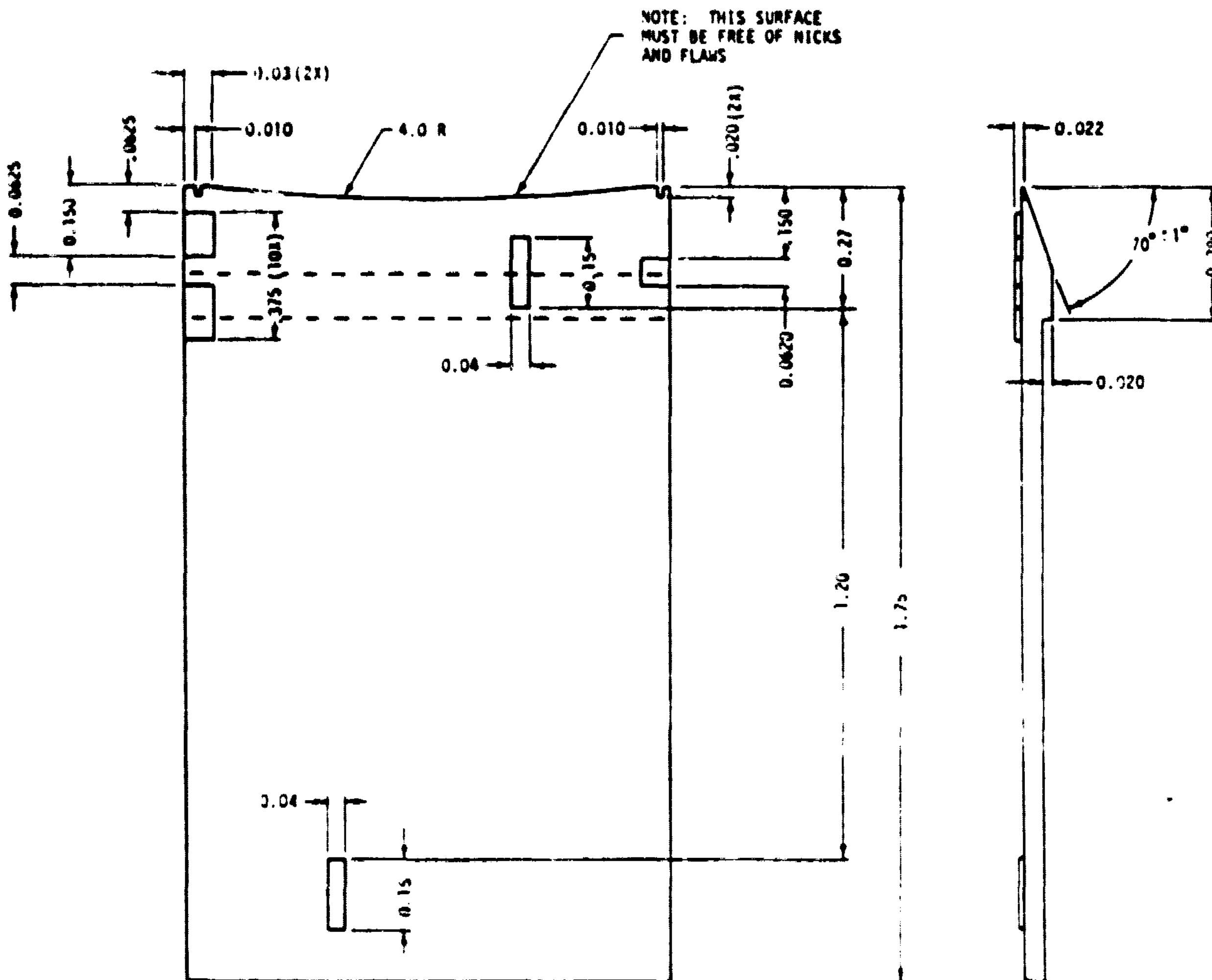

NOTES:

1. UNLESS OTHERWISE NOTED ALL DIMENSIONS ARE IN INCHES
2. TOLERANCES UNLESS OTHERWISE NOTED:
   2 PLCS. = 0.01
   3 PLCS. = 0.003
3. TWO IDENTICAL PARTS REQUIRED

EAGLE-PICHER INDUSTRIES, INC. SPECIALTY MATERIALS DIVISION		
TWO PIECE DIE		
SCALE APPROXIMATELY 4" = 1"	DATE 4 SEPT 73	
DRAWN JHF		
	DRAWING NO.	EXHIBIT 1 TO CONTRACT NO 354877

Figure 38. JPL Suggested Two Piece Die Design

The one-piece ceramic die machining experience showed that it was necessary to increase the body thickness in order to enhance the survival rate in the slot sawing operation. Fractures occurred, for the thin bodied dies, at the root of the saw kerf due to the wedging action of the blade. It was also necessary to move the edge defining slots, at the top of the die, inboard in order to make the "ears" less susceptable to breakage.

Due to problems encountered in the coating operation, described later in this section, it was necessary to fabricate two-piece dies from hot pressed ceramic blanks. The need to modify the JPL suggested design, Figure 38, was recognized immediately. This design was based upon utilization of a milling operation and required adaptation to a grinding operation. The need for lateral restraint was deemed to take precedence over the need for longitudinal restraint when the mating halves were assembled.

The two-piece die design shown in Figure 39 was suggested by Eagle-Picher and approved by JPL. It was designed for a proper fit with a 0.005" thickness of CNTD coating in place. Two-piece dies were successfully ground to Figure 39 dimensions from hot pressed blanks of both and Si_3N_4.

The CNTD coating techniques were first applied to dies of the one-piece design, Figure 37, using the Si_3N_4 deposition process. The application of a uniform coating of CNTD material to the inner surfaces of the die slot was anticipated to become a difficult task, and graphite development die shapes were prepared (HLM grade). The use of graphite lowered the fabrication costs dramatically and allowed fourteen development dies to be furnished to Chemetal Corporation for coating efforts described as follows.

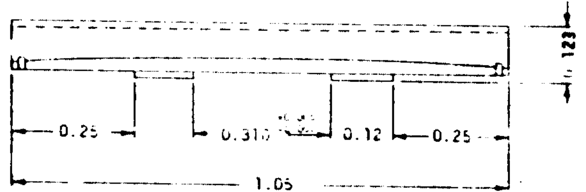

EAGLE-PICHER INDUSTRIES, INC.		
SPECIALTY MATERIALS DIVISION		
TWO PIECE DIE PART A, REV 1		
SCALE 4" = 1"		DATE 5 JANUARY 1979
DRAWN JMF	CHECKED	APPROVED
SHEET 1 of 2	DRAWING NO MRLCS-62, REV 1	

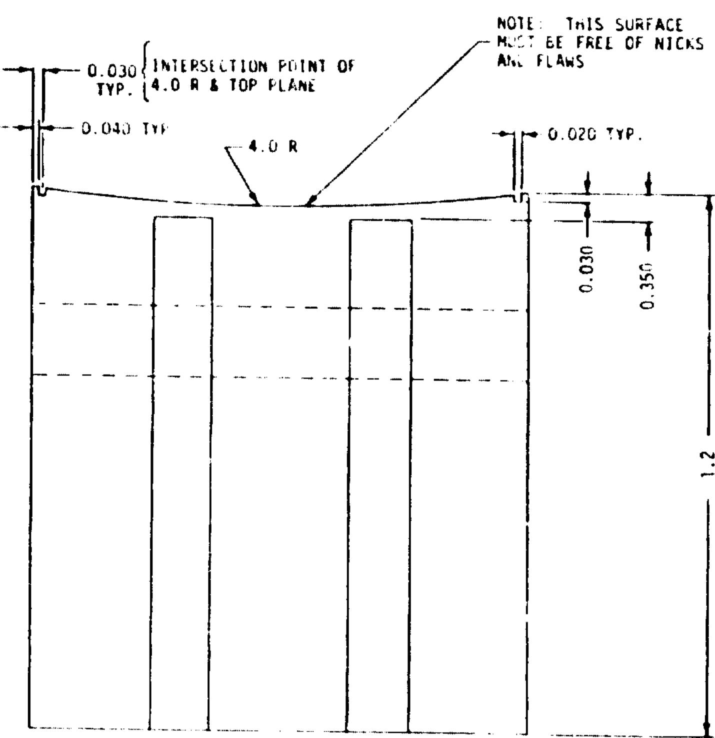

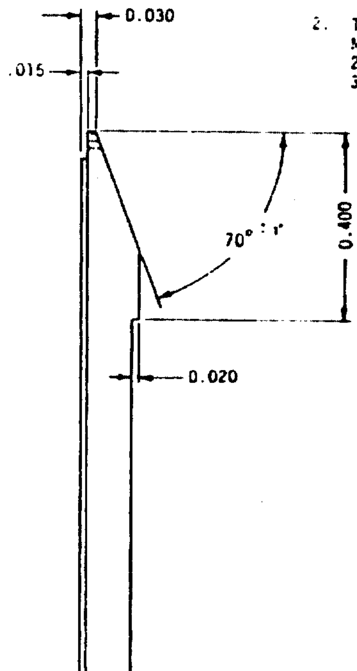

NOTES:
1. UNLESS OTHERWISE NOTED ALL DIMENSIONS ARE IN INCHES
2. TOLERANCES UNLESS OTHERWISE NOTED:
2 PLCS. = 0.01
3 PLCS. = 0.003

Figure 39-a). Eagle-Picher Modified Two Piece Die Design, Part A

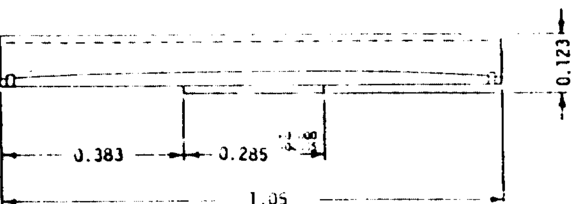

EAGLE-PICHER INDUSTRIES, INC.		
SPECIALTY MATERIALS DIVISION		
TWO PIECE DIE PART B, REV 1		
SCALE 4" = 1"		DATE 4 JANUARY 1979
DRAWN JMF	CHECKED	APPROVED
SHEET 2 of 2	DRAWING NO. MRLCS-63, REV 1	

NOTES:
1. UNLESS OTHERWISE NOTED ALL DIMENSIONS ARE IN INCHES
2. TOLERANCES UNLESS OTHERWISE NOTED:
   2 PLCS. = 0.01
   3 PLCS. = 0.003

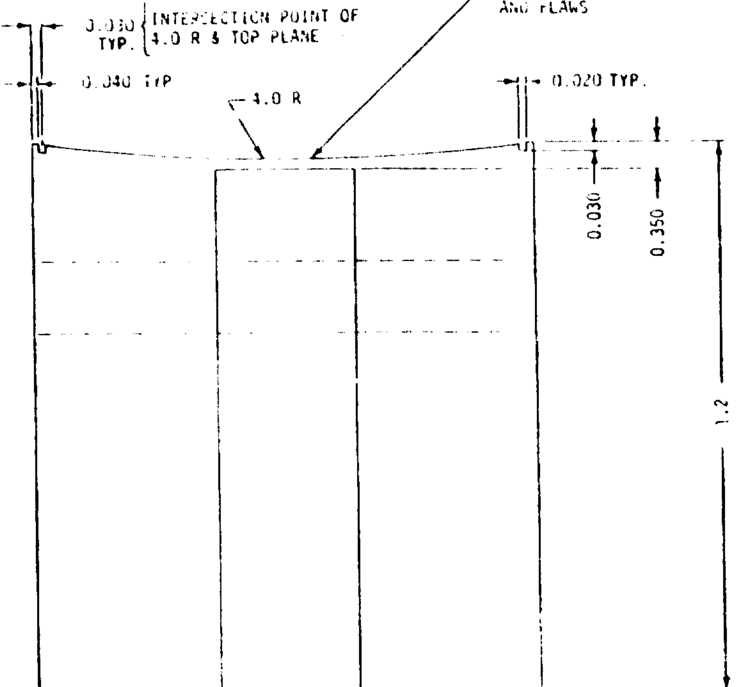

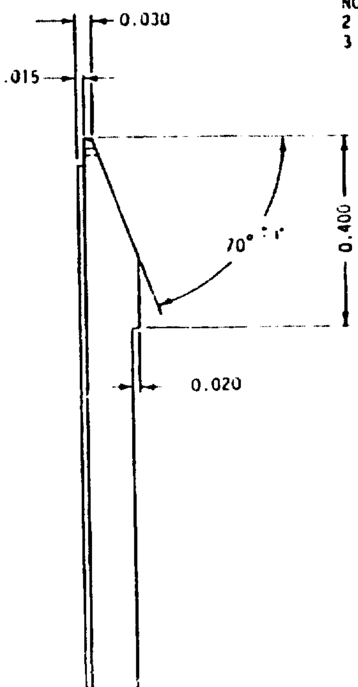

Figure 39-b). Eagle-Picher Modified Two Piece Die Design, Part B

Using deposition conditions similar to those used for coating the silicon nitride containers, initial experimental runs were made in a three inch diameter graphite reactor. Deposits were not uniform, especially in the area of the "slot". Several attempts were made, with increased diluent concentrations, to increase gas velocity. Sectioned experimental parts revealed excessive build-up on the edges of the part with thin deposits extending approximately two-thirds the depth of the slot.

Secondly, a two inch diametric furnace was used to further increase gas velocity and "force" reactant gases through the slot area. Thirdly, a rectangular gas injector was designed and installed to direct the gas stream more accurately, taking into account the geometry of the part. Fourthly, gas velocities, diluent concentrations, and reactive gas partial pressures were altered in an attempt to improve uniformity. The steps described above were evaluated singularly and in combination, with similar results.

Other experiments were conducted using a "throttle exhaust", thereby attempting to increase the velocity of the exiting gases while maintaining a more viscous flow in the area of the part. The orientation of the part was also altered so that the slots would be presented normal and diagonally to the gas stream. All such attempts provided only marginal improvements in results.

All the above work was conducted on graphite substrates as pointed out earlier. After the tests described above were conducted, the staff at Chemetal contacted Eagle-Picher to inform them that the probability of obtaining a uniform deposit of silicon nitride on the actual hardware was low. Eagle-Picher then directed Chemetal to return the uncoated hardware and all coated graphite experimental parts.

The experimental parts were evaluated and the obvious decision to utilize the suitably modified two-piece die (Figure 39) was made. Unfortunately the efforts to achieve the uniform coating of a one-piece die had exceeded the manhour and material allocations for this item and two-piece dies of Si_3N_4 w/4 wt% MgO have been delivered without the CNTD Si_3N_4 coating.

CNTD SiC was successfully applied to hot pressed and ground blanks of SiC w/1 wt% B (Figure 39, two-piece die) after brief experiments with graphite shapes. The coatings were 0.005" thick, β-SiC by x-ray diffraction, and exhibited morphology similar to the test specimens, Figure 2. An assembled pair of two-piece CNTD SiC coated die halves are shown in Figure 40. All surfaces are coated excepting three small areas where a fine diameter tungsten wire "spider" supported each piece during separate depositions. Three CNTD SiC coated die sets were delivered under the contract.

3. MANUFACTURING COST PROJECTIONS

The following cost analyses are based upon the incorporation of the technology developed in this program. Projections have been included, in addition, which take into account process modifications utilizing alternative lower cost ceramic fabrication techniques. These lower cost ceramic substrates would be higher in porosity than the hot pressed articles developed to date, but would perform in a comparable manner if coated with the CNTD material. They would still offer substantial advantages, such as coefficient of thermal expansion matching and minimal influence on P_{O_2}, over graphite substrates.

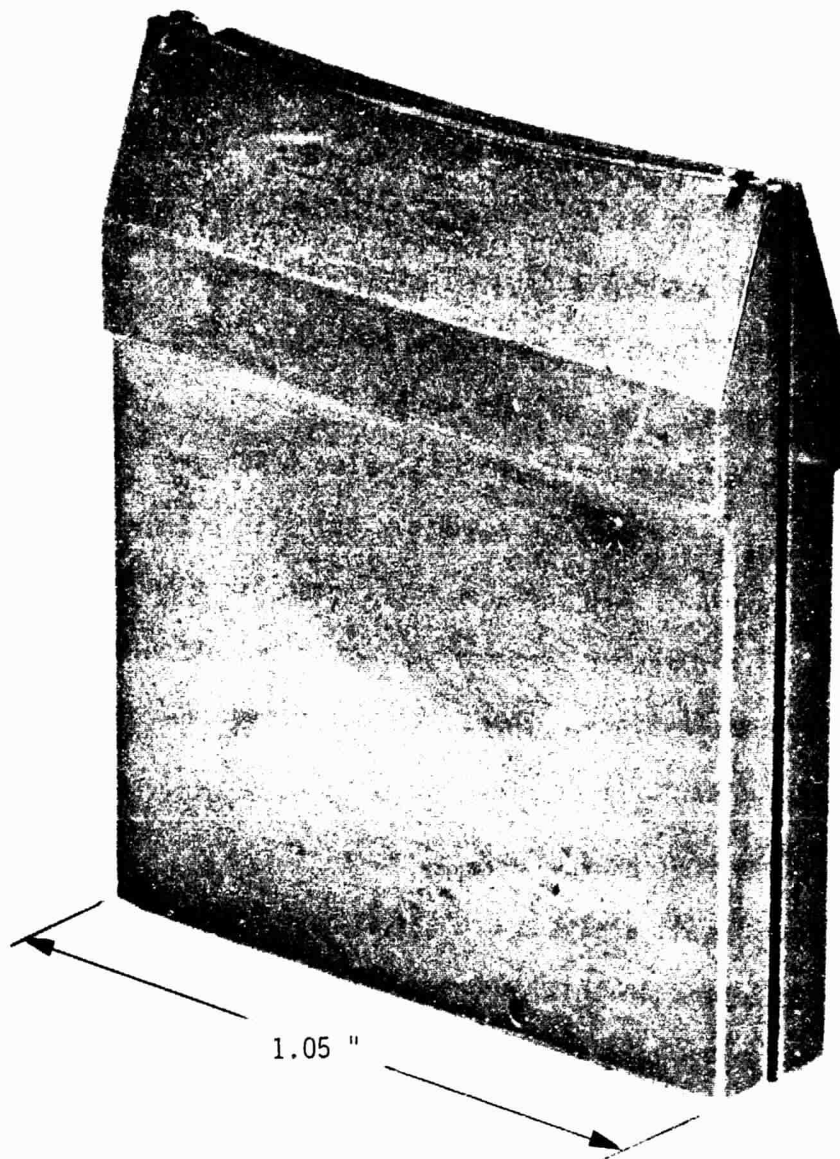

Figure 40. CNTD SiC Coated SiC (w/1 wt% B)
Two Piece Die, Assembled

3.1 CONTAINER MANUFACTURING PROJECTIONS

The cost projections, based upon manufacturing 100,000 units per year, were computed using equation (1) below, from the Solar Array Manufacturing Industry Costing Standards (SAMICS)*.

Equ. (1)

$$\text{Price} = \frac{0.49(\text{EQPT}) + 97(\text{SQFT}) + 2.1(\text{DLAB}) + 1.3(\text{MATS}) + 1.3(\text{UTIL})}{\text{Quantity}}$$

Where:

EQPT = Cost of all the equipment,

SQFT = Floor space required by the equipment,

DLAB = Annual cost of all direct labor,

MATS = Annual cost of all direct materials and supplies,

UTIL = Annual cost of all direct utilities.

The proposed manufacturing sequence is shown in Figure 41. The crucibles fabricated for the present program were manufactured by hot pressing. One cost saving alternative shown in Figure 41 is that of forming green bodies from powders under pressure at room temperature then heating in the appropriate atmosphere to consolidate the body. In the case of Si_3N_4 articles the green body could consist of Si_3N_4 powder with the appropriate sintering aids or could consist of elemental silicon which would be heated in nitrogen atmosphere to form reaction bonded silicon nitride (RBSN). The latter process would obviate extremely high temperature furnacing, resulting in a lower priced article. In a second alternative, the isostatic pressing sequence shown in Figure 41 would be

---

* R.W. Aster and R.G. Chamberlain, Interim Price Estimation Guidelines: A Precursor and an Adjunct to SAMIS III, JPL Document 5101-33, Jet Propulsion Laboratory, Pasadena, Calif. (1977).

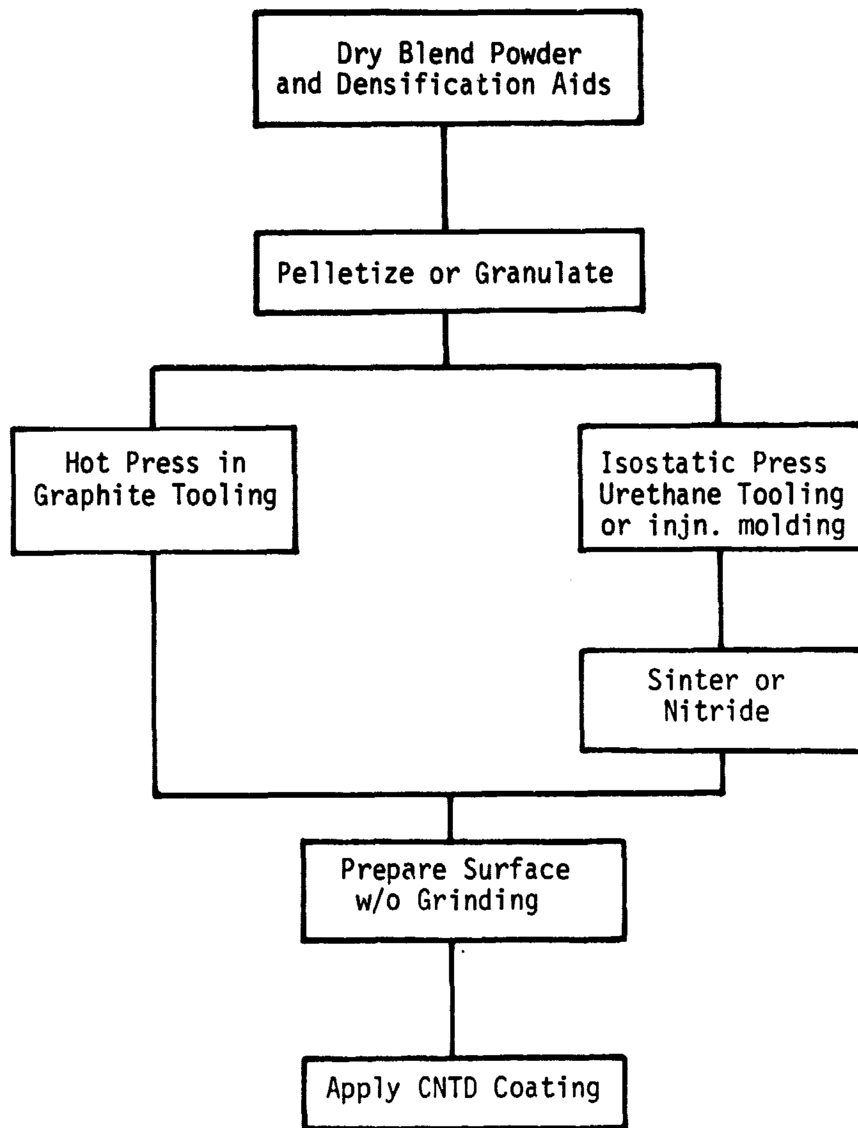

Figure 41. Container Manufacturing Process

replaced by an injection molding operation, with appropriate changes in the powder preparation portion of the diagram.

A summary of the capital equipment requirements for producing 100,000 containers per year is given in Table V, and a total cost summary is presented in Table VI, with the cost per unit shown in the extreme right hand column. The facility is projected to operate three shifts per day for 350 days per year with a direct labor cost of $6.00/hr. For the hot pressing scenario graphite tooling costs are projected to be $1,000,000.00/yr.; CNTD precursor gas costs are $5,200.00/yr.; and each container will require a nominal 200g of powder. It is readily apparent that graphite hot press tooling costs are a prime driver and that the use of alternative forming techniques is desirable.

Scenario number one represents a scale up of present hot press operation using raw materials comparable to those used in the present study. Scenario number four represents the incorporation of low cost forming as well as low cost raw materials. The $0.285/lb material cost is based upon the current (1979) price for a SiC powder which is of sufficient quality to merit consideration for fabricating a substrate to be coated with a pure coating. Other scenarios could be developed which would give intermediate price values, however these four are presented in order to define the reasonable bounds of achievable costs.

3.2 DIE MANUFACTURING PROJECTIONS

Die manufacturing would proceed according to the flow diagram shown in Figure 41 with the addition of a diamond grinding operation prior to preparing the surface for CNTD coating. The costs were projected once again using equation (1) and allowing for lower cost substrate

TABLE V

Container Manufacturing Capital Equipment Requirements[1]

EQUIPMENT	COST
Mill 200 lb. cap. ball mill or high intensity high throughput dry blender	$ 30,000
Granulation or Pelletization	$ 6,000
Hot Press vacuum, induction heated semicontinuous, (3 reg. @ 100 K $/ea)	$300,000
(Alternate to Hot Press) rapid cycle isostatic press or injn. mold plus vacuum/inert/N_2 sintering furnace	($140,000)
CNTD Coating Deposition Chamber	$110,000

1. For production of 10^5 units per year

TABLE VI

Container Manufacturing Cost Summary

SCENARIO	EQPT (K$)	SQFT (ft^2)	DLAB (K$)	MATS (K$)	UTIL (K$)	COST/UNIT[1] ($)
1. Hot Press $32.00/lb powder 9 mndays/calendar day	446	5000	151.2	2,413.2	53	42.27
2. Hot Press $12.50/lb powder 9 mndays/calendar day	446	5000	151.2	1,555.2	53	31.12
3. Isopress & Sinter/Nitride $12.50/lb powder 4 mndays/calendar day	286	3000	67.2	655.2	27	14.40
4. Isopress & Sinter/Nitride $0.285/lb powder 4 mndays/calendar day	286	3000	67.2	12.5	27	6.24

1 For production of 10^5 units per year as per Equation (1) below:

$$\text{Price} = \frac{0.49\ (\text{EQPT}) + 97\ (\text{SQFT}) + 2.1\ (\text{DLAB}) + 1.3\ (\text{MATS}) + 1.3\ (\text{UTIL})}{\text{QUAN}}$$

fabrication techniques. The facility is projected to operate one eight hour shift per day for 250 days per year with a direct labor cost of $6.00/hr. For the hot pressing scenario graphite tooling costs are projected to be $300,000.00/yr.; CNTD precursor gas costs are $600.00/yr.; diamond abrasive wheel replacement is $12,000.00/yr.; and each die pair will require a nominal 25 g of powder. The use the alternate forming techniques would replace the $300,000.00 graphite hot press tooling with $40,000.00 worth of hardened steel or carbide and allow forming to near net shape. The capital expense for grinding equipment and the replacement diamond abrasive cost were therefore reduced 50%. The capital equipment cost is shown in Table VII and the die manufacturing cost summary in Table VIII.

The two-piece die shape (Figure 38) is rather complex. Further cost reductions would be possible if the geometry could be simplified. The die is especially without geometric simplification, an ideal candidate shape for injection molding and nitridization of elemental silicon to yield an RBSN substrate for CNTD Si_3N_4 coating. This technology has been proven, in the gas turbine research programs, to yield parts of very near net shape with minimal dimensional change or warpage during processing.

4. CONCLUSIONS

1) The CNTD process is capable of producing dense, fine grained coatings of molten silicon resistant ceramic, providing a great improvement in contrast with uncoated hot pressed samples of the same nominal chemical composition.

TABLE VII

Die Manufacturing Capital Equipment Requirements[1]

EQUIPMENT	COST
Mill 200 lb. cap. ball mill or high intensity high throughput dry blender	$ 30,000
Granulation or Pelletization	$ 6,000
Hot Press vacuum, induction heated semicontinuous	$100,000
(Alternate to Hot Press) uniaxial compacting press, extrusion press, or injection molding equip.; plus vacuum/inert/N_2 sintering furnace	($140,000)
Horizontal Surface Grinders 12 req. @ $20,000/ea.	$240,000
CNTD Coating Deposition Chamber	$110,000

[1]For production of 10^5 units (ea. unit consists of two halves) per year.

TABLE VIII

Die Manufacturing Cost Summary

SCENARIO	EQPT (K$)	SQFT (ft^2)	DLAB (K$)	MATS (K$)	UTIL (K$)	COST/UNIT[i] ($)
1. Hot Press $32.00/lb powder 5 mn day/calendar day	486	4000	60	489	17.7	14.11
2. Hot Press $12.50/lb powder 5 mn day/calendar day	486	4000	60	381.5	17.7	12.71
3. Uniaxial or Extrusion Press or injection mold $12.50/lb powder 3 mn day/calendar day	406	3000	36	115.5	17.7	7.39
4. Uniaxial or Extrusion Press or injection mold $0.265/lb powder 3 mn day/calendar day	406	3000	36	48.2	17.7	6.51

[i] For production of 10^5 die pair per year as per Equation (1) below:

$$\text{Price} = \frac{0.49(\text{EQPT}) + 97(\text{SQFT}) + 2.1(\text{DLAB}) + 1.3(\text{MATS}) + 1.3(\text{UTIL})}{\text{Quantity}}$$

2) The coating/substrate combinations have proven to be thermomechanically stable and compatible.

3) Of the samples tested, CNTD coated SiC appears to have the highest resistance to molten silicon attack.

4) Of the three CNTD coatings tested, SiC is most wetted, exhibits the greatest stability of contact angle with time and is the most sensitive to changes in oxygen partial pressure in the range investigated.

5) The contact angle of molten silicon measured on the samples as a function of time at a fixed P_{O_2} decreased, more rapidly at first, tending toward a constant small rate of change after 1 hour.

6) Increasing the oxygen partial pressure increases the contact angle, apparently because adsorbed oxygen lowers the solid-vapor interfacial free energy.

7) Adsorbed oxygen increases the degree of attack of molten silicon on CNTD coated SiC, Si_3N_4, and AlN. The effect is minimized by allowing the solid surfaces to equilibrate with the low P_{O_2} environment prior to melting.

8) Prototypic containers and dies have been fabricated from the materials systems developed and the development of cost effective, high volume production methods appears to be obtainable.

5. RECOMMENDATIONS FOR FUTURE WORK

1) Investigate the effects of oxygen partial pressure upon the performance of conventional refractory materials in contact with molten silicon. This would include chemical vapor deposited (CVD) materials not fabricated by the specialized CNTD process.

2) Fabricate ceramic container and die substrates by lower cost methods as discussed in section 3, coat with CNTD coatings, and test in silicon ribbon production.

APPENDIX A

GENERAL APPEARANCE OBSERVATIONS AND X-RAY DIFFRACTION RESULTS FOR COATINGS

TABLE	PAGE
TABLE A - I, CMS-1	A-1
TABLE A - II, CMS-2A	A-3
TABLE A - III, CMS-2B	A-5
TABLE A - IV, CMS-3	A-7
TABLE A - V, CMS-4A	A-8
TABLE A - VI, CMS-4B	A-9

TABLE A-I

General Appearance Observations and X-Ray Diffraction Results, CNTD SiC Coatings on SiC Substrates (CMS-1)

Specimen Designation	Coating Thickness	Chemetal Observations	MRL X-Ray Diffrac. Results Morphology/Phases Present
1-4304-28-028	.0060"	Very fine crystals, slightly green tint, good deposit	Strong crystalline β-SiC plus an unknown peak possibly represent a minor crystalline phase or super structure and a low angle, low intensity diffuse peak
-29	.0069"	Rough surface, smoother than R28 deposit had a bluish-black color (shiny)	" " "
-30	.0069"	Smoother surface, deposit is a dull bluish-black color	" " "
-31	.0130"	Smooth, shiny, reflective surface but still a little bumpy	Except no diffuse peak
-32	.0218	Shiny, rough surface with a darker deposit on the outer radius	" " "
-33	.0083"	Very smooth surface but a little dull	Except no diffuse peak
-34	.0059"	Smooth surface and slightly reflective surface	" " "
-35	.0086"	Very bumpy surface, not a good deposit, extremely uneven deposit, dark & dull on appearance	" " "
-36	.0130"	" " "	" " "
-37	.0153"	Smooth, dark and reflective surface, good deposit	" " "

TABLE A-I - continued

Specimen Designation	Coating Thickness	Chemetal Observations	MRL X-Ray Diffrac. Results Morphology/Phases Present
1-4303-39-098	.0070"	Slightly rough deposit, had a dull surface	" " "
-40	.0083"	Rather smooth surface, slightly reflective	" " "
-41	.0176"	Appearance same Run #40	" " "
-42	.0072"	Smooth, dark, reflective deposit	" " "
-43	.0096"	Smooth, shiny, slightly reflective deposit, light bluish-black color	" " "

TABLE A-II

General Appearance Observations and X-Ray Diffraction Results, CNTD Si_3N_4 Coatings on Si_3N_4 (w/4wt/o MgO) Substrates(CMS-2A)

Specimen Designation	Coating Thickness	Chemetal Observations	MRL X-Ray Diffrac. Results Morphology/Phases Present
8-4306-264-021	0.011"	glassy amorphous, slightly bumpy, yellowish brown color	amorphous/no crystalline peaks visible
-265		coating did not bond, see run #270 below	→ see remarks below
-266	0.011"	full crystalline deposit	anomalous crystalline pattern
-267	0.005"	crystalline deposit, clear yellow in center, darker on edges	crystalline/strong α-Si_3N_4 possible β-Si_3N_4
-268	0.010"	smooth amorphous with some crystalline regions	amorphous/devitrifying to α-Si_3N_4
-269		full crystalline deposit	→ to JPL
-270		full crystalline deposit	crystalline/very strong α-Si_3N_4, possible β-Si_3N_4
-271	0.0086"	crystalline surface changing to amorphous near substrate	crystalline/strong α-Si_3N_4, possible β-Si_3N_4
-272	0.014"	amorphous-glassy, bumpy deposit	amorphous/no crystalline peaks visible
-273	0.0165"	crystalline deposit yellowish color in center	crystalline/strong α-Si_3N_4, possible β-Si_3N_4
-274	0.0087"	crystalline deposit, smaller grains than previous runs	crystalline/strong α-Si_3N_4, possible β-Si_3N_4

TABLE A-II - continued

Specimen Designation	Coating Thickness	Chemetal Observations	MRL X-Ray Diffrac. Results Morphology/Phases Present
8-4306-275-021	0.011"	small grains, crystalline translucent, smooth deposit	crystalline/strong α-Si_3N_4, possible β-Si_3N_4
-276		small grains, smooth translucent deposit	→ to JPL
-277	0.016"	amorphous/crystalline mixture	amorphous/mostly devitrified to α-Si_3N_4
-278	0.017"	crystalline deposit, possibly cracked	mostly crystalline pattern/ α-Si_3N_4 present almost total devitrification
-279	0.0106"	small grains, smooth deposit	crystalline/α-Si_3N_4 + unknown pattern
-280		small grained deposit, crystalline facets visible	→ to JPL

TABLE A-III

General Appearance Observations and X-Ray Diffraction Results, CNTD Si_3N_4 Coatings on Si_3N_4 (w/4wt/o MgO) Substrates(CMS-2B)

Specimen Designation	Coating Thickness	Chemetal Observations	MRL X-Ray Diffrac. Results Morphology/Phases Present
1-4305-22-098	0.0057"	very fine crystals, slightly green tint, good deposit	crystalline/strong α-Si_3N_4, weak β-Si_3N_4
-23	0.0052"	very fine crystals same as #22 (PART #3)	crystalline/strong α-Si_3N_4, possible β-Si_3N_4
-24	0.0053"	large crystals, deposit very uneven	crystalline/strong α-Si_3N_4, very weak β-Si_3N_4
-25	0.0044"	small crystals, deposit very uneven	amorphous/devitrifying to α-Si_3N_4 possible presence of β as well
-26	0.0055"	large crystals, even deposit, good deposit	crystalline/strong α-Si_3N_4, possible β-Si_3N_4
-27	0.0047"	small crystals, even deposit	→ to JPL
-28	0.0079"	larger crystals than #27 (PART #8), even deposit	→ to JPL
-29	0.0088"	semi amorphous/semi crystalline, small crystals	anomalous pattern-possibly amorphous
-30	0.0049	clear deposit, non crystalline, smooth, cracks visible	amorphous/devitrification just starting no identification of phase (s)
-32	0.0107	medium size crystals with some cracks visible	amorphous/anomalous pattern
-33	0.0059	small crystals, cracks visible	crystalline/strong α-Si_3N_4, possible β-Si_3N_4

TABLE A-III - continued

Specimen Designation	Coating Thickness	Chemetal Observations	MRL X-Ray Diffrac. Results Morphology/Phases Present
1-4305-34-098	0.0059"	small crystals, even deposit (no cracking visible)	crystalline/strong α-Si_3N_4, possible β-Si_3N_4
-35	0.0096"	medium size crystals, translucent deposit	crystalline/strong α-Si_3N_4, no β-Si_3N_4 noticeable
-36	0.0094"	large crystals, very translucent deposit	crystalline/strong α-Si_3N_4, no β-Si_3N_4 noticeable
-37	0.0106"	large crystals, slightly green color, good deposit	→ to JPL

TABLE A-IV

General Appearance Observations and X-Ray Diffraction Results, CNTD AlN Coatings on AlN Substrates (CMS-3)

Specimen Designation	Coating Thickness	Chemetal Observations	MRL X-Ray Diffrac. Results Morphology/Phases Present
1-4323-06-098	0.0038"	Even deposit of medium size crystals, greenish color	Hexagonal AlN, three unknown weak peaks, 102 and 103 peaks considerably higher than expected
-07	0.0228"	Black, even deposit of large crystals	As above
-08	0.0072"	Even deposit of small crystals, reddish brown color	As above
-09	0.0063"	Small crystals, brown at center and green at edges	As above
-10	0.0062"	Very fine grain, small crystals, evenly deposited	As above
-11	0.0146"	Medium size crystals with reddish-green color	As above
-12	0.0157"	Even deposit, medium size crystals	As above, relative intensity affectation quite strong
-14	0.0122"	Same as run 13	As above
-16	0.0086"	Small crystals, evenly deposited. Deposit cracked	As above, two unknown peaks
-17	0.0112"	Small crystals, evenly deposited, good deposit	One unknown peak, relative intensity affectations strongest of all samples
-18	0.0101"	Small crystals, similar to run 17	Two unknown peaks, very strong relative intensity affectations

TABLE A-V

General Appearance Observations and X-ray Diffraction Results, Altered Si_3N_4, Si_2ON_2 Attempt, on Si_3N_4 (w/10wt% Y_2O_3), Substrate, (CMS-4A)

Specimen Designation	Coating Thickness	Chemetal Observations	MRL X-Ray Diffraction Results
1-4323-43-098	0.0032"	Deposit was amorphous with very fine cracks	Amorphous, no peaks
-44	0.0071"	Fine crystals in Center, 1/8" O.D. rim amorphous	α-Si_3N_4
-45	0.0066"	Deposit very similar to run #44, but larger crystals	α-Si_3N_4
-46	0.0061"	Very fine crystals in center area with amorphous at outer diameter	α-Si_3N_4
-47	0.0061"	Same as run #44	α-Si_3N_4
-48	0.0061"	Crystalline deposit, smaller crystals in center	α-Si_3N_4
-51	0.0058"	Similar to run #48	α-Si_3N_4; possible amorphous phase present

TABLE A-VI

General Appearance Observations and X-Ray Diffraction Results, Altered Si_3N_4, SiAlON Attempt, on Si_3N_4 (w/10wt% Y_2O_3) Substrate, (CMS-4B)

Specimen Designation	Coating Thickness	Chemetal Observations	MRL X-Ray Diffraction Results
1-4323-49-098	0.0057"	Amorphous with fine cracks	Amorphous, no peaks
-50	0.0042"	Same as run 49	" " "
-52	0.0053"	Amorphous with network cracks	" " "
-54	0.0142"	Center contained crystals outer diameter was bumpy	α-Si_3N_4
-62	0.0139"	Large black crystals in center, very large black nodules on outside	α-Si_3N_4
-65	0.0127"	Amorphous deposit with crystalline nodules	α-Si_3N_4, possible amorphous phase present
-67	0.0141"	Fine crystals at center with larger crystalline nodules near O.D.	α-Si_3N_4
-68	0.0104"	Amorphous deposit with crystalline nodules	α-Si_3N_4
-69	0.0105"	About 1/8" near O.D. crystalline with center amorphous with a few larger crystalline nodules	α-Si_3N_4, possible amorphous phase present
-70	0.0129"	All fine crystals	α-Si_3N_4
-71	0.0144"	All fine crystals	α-Si_3N_4

APPENDIX B

DETAILED DISCUSSION OF THE X-RAY DIFFRACTION CHARACTERIZATION OF THE ALTERED Si_3N_4 COATINGS (CMS-4A and 4B)

APPENDIX B

DETAILED DISCUSSION OF THE X-RAY DIFFRACTION CHARACTERIZATION OF THE ALTERED Si_3N_4 COATINGS (CMS-4A and 4B)

B.1 PEAK IDENTIFICATION

CMS-4A and 4B coatings were analyzed by x-ray diffraction using Cu_{K_α} radiation from 2Θ equals 0° to 100°. However, due to modification of the sample holder for the coated substrates, the low angle beam was totally blocked for 2Θ angles less than 16°.

Both coating materials were checked against the ASTM card files for Si_2ON and Si_2ON_2 using data obtained from the literature[1] and for α - Si_3N_4 and β - Si_3N_4 using computed powder x-ray diffraction data from an AMMRC report[2]. Only α - Si_3N_4 was detected in the coatings. Several coatings from each lot showed no peaks and were probably amorphous while others showed a higher than normal background indicating the possible presence of some amorphous material. Tables A-V and A-VI of Appendix A lists these results.

No unknown peaks were detected for $2\Theta < 60^o$ and no significant unknown peaks were detected at higher angles. One of the variances noted was that all peaks on both the substrates and coatings deviated in 2Θ angle from the computed data of AMMRC. This same effect was noted on all previous coatings analyzed by x-ray diffraction. The peaks were consistently at a lower angle than expected, with the largest displacement occurring at low angles with decreasing displacements occurring as the angle increased but never reaching zero displacement. The actual displacement was not consistent from sample to sample and varied from 0.2^o to 0.7^o at low angle ($\sim 30^o$) down to 0.1^o to 0.3^o at the highest angle ($\sim 100^o$). A lattice parameter change could possibly

cause an angular displacement of the peaks but this displacement would normally be expected to vary in the opposite manner (largest at the higher angles) and was therefore not considered to be a probable explanation of the observed effect. The alignment of the x-ray diffractometer was determined to be well within specification and Si_3N_4 powder, using the standard powder mounting procedure, did not show any angular displacement of the peaks.

In an effort to determine the origin of these displacements, an x-ray diffractometer at Pittsburg State University, Pittsburg, Kansas, was used to run a sample which had shown large angular displacement. After careful alignment of the machine at P.S.U., this sample showed all peaks to be within 0.1^{o} of the values listed by AMMRC. The displacement problem is now considered to be a mechanical alignment problem not associated with the coating and that lattice parameter changes, if present, were not detected.

B.2 RELATIVE INTENSITIES

Two x-ray diffraction scans were made for each coating sample without demounting. The sensitivities of the two scans were adjusted to a ratio of one to five enabling the more intense peaks to remain on scale for intensity measurements while also allowing lower intensity peaks to be detected. Peak intensities could then vary by a factor of approximately 100 and still be measurable.

As experienced, to a lesser degree, with the CMS-2 coating materials, the measured relative intensities did not agree with the literature (in this case the AMMRC calculated intensities). The ratios of the observed to expected intensities were estimated to be

as much as a factor of 20 in individual cases but were more commonly near 10. The samples of CMS-4A showed some consistency in the particular peaks that were high and low whereas, samples from CMS-4B showed much less consistency. Table B-I lists the AMMRC calculated relative intensities and the experimental intensities for two coatings of CMS-4A and one coating of CMS-4B.

Only the calculated relative intensities greater than one are included in Table B-I. The experimental intensities have been normalized so that the sum for one coating is equal to the sum of the calculated intensities. The first two experimental columns are typical of CMS-4A and show several peaks that were consistently high and several that were consistently low. This degree of regularity was not noted in the samnles from CMS-4B. It should be noted, however, that the (100) peak would not be detectable because of the obstruction of the x-ray beam by the mount and that other low angle lines could have been at least partially affected by this same feature. When three of the specimens were run on the x-ray machine at P.S.U., the (100) peak was still not detectable and the other low angle peaks did not seem significantly different in intensity. For all CMS-4A specimens run at both MRL and at P.S.U. the (222) line was the most intense. This, however, was not generally true of those from CMS-4B. Table B-II gives the calculated (from AMMRC) and experimental (run at P.S.U.) ratios of the intensities of the (222) peak to the five calculated most intense peaks. These are for two specimens (one from CMS-4A and one from CMS-4B) that were run repeatedly at different surface positions and orientations. The experimental ratios are significantly larger than the calculated ratios.

TABLE B-I

Calculated and Experimental Intensities
(CMS-4)

hkl	Calculated Intensity*	Experimental Intensity CMS-4A # 46	CMS-4A # 47	CMS-4B # 62
100	15	0	0	0
101	100	6	3	20
110	48	11	0	1
200	32	6	1	4
201	99	54	38	83
002	11	0	1	19
102	89	9	5	79
210	90	54	1	9
211	66	115	63	26
112	3	6	20	6
300	2	2	0	2
202	38	8	11	36
301	42	44	25	10
220	5	2	0	0
212	8	3	10	6
310	8	8	0	20
103	11	0	0	35
311	17	38	31	12
302	1	**	**	**
203	8	2	1	32
222	22	192	230	140
312	3	11	19	5
320	3	0	0	1
213	5	8	21	11
321	31	27	2	10
410	1	**	**	6
402	1	**	**	**
303	26	7	12	22
411	25	39	7	10
004	14	0	0	20
104	4	0	0	7

TABLE I (cont.)

hkl	Calculated Intensity*	Experimental Intensity CMS-4A # 46	CMS-4A # 47	CMS-4B # 62
322	32	128	140	83
500	1	**	?	**
313	8	?	?	?
114	5	?	?	?
501	6	8	0	0
412	20	21	10	25
204	4	?	?	?
330	11	8	0	?
420	3	3	0	0
421	6	11	3	6
214	9	3	4	20
502	2	2	1	1
510	2	0	0	1
323	12	69	150	83
511	6	?	0	1
332	2	8	9	8
422	4	15	17	25
413	8	?	?	?
224	1	**	**	1
314	2	0	2	2
512	4	3	0	3
430	3	3	0	2
503	1	**	**	**
431	2	1	0	2
520	1	**	**	**
205	3	0	2	9
521	1	**	**	**
423	4	12	40	12
324	5	11	69	19
610	2	?	0	?
513	5	7	67	6
611	4	4	0	1

* For α Si_3N_4 from AMMRC Report

** Calculated intensity too low to be detectable at normal experimental intensity

? Peak intensity not discernable

TABLE B-II

Ratios of (222) Peak Intensities to Five Strong Peaks[a]

Peak Comparison	Calculated[b] Ratio	Experimental Ratios					
		Pattern 1A[c]	Pattern 2A	Pattern 1B[d]	Pattern 2B	Pattern 3B	Pattern 4B
(222)/(101)	22%	280%	260%	>220%	150%	280%	>230%
(222)/(201)	22%	115%	180%	>910%	200%	140%	>380%
(222)/(102)	25%	1330%	*	>1000%	330%	430%	>1100%
(222)/(210)	24%	440%	560%	**	**	**	**
(222)/(211)	33%	310%	320%	>1000%	450%	410%	>590%

* The (102) peak missing

** The (210) peak missing or not intense enough to be measurable.

a As measured from patterns run at Pittsburg State University of Pittsburg, Kansas

b From the AMMRC report

c Patterns 1A and 2A both made on coating 1-4323-44-098 of CMS-4A at different orientations.

d Patterns 1B thru 4B all made on coating 1-4323-70-098 of CMS-4B at various positions and orientations.

These intensity variations could possibly be explained by an oriented growth pattern, a non-uniformity of crystallite size, a change in the structure factor due to non-stoichiometry, limited incorporation of Al and O atoms into the α - Si_3N_4 structure as interstitials or as substitutions for Si and N respectively, or any combination of these. Although a complete investigation could not be made, it was suggested[3] that a quick method was available that might provide more insight to the situation.

A Laue camera, (Figure B-I) normally used to orient single crystals, was used with unfiltered copper radiation. Spots appear on the film when the Bragg condition is met for a given plane and one particular wavelength of the impinging continuous or polychromatic radiation. When a randomly oriented polycrystalline substance is used for the sample, all planes will find a wavelength of radiation that will satisfy the Bragg condition for their particular orientation and the film should show a large number (at least one for every reflecting plane) of randomly oriented spots. However, since there is also a characteristic radiation present (the K_α and K_β lines) that may be more intense (as is the case here) than the continuous radiation, the spots due to the characteristic radiation will form pronounced circular rings. These would be from those planes having the proper orientation and d-spacing to meet the Bragg condition for the $Cu_{k\alpha}$ or K_β wavelergth. If the incident x-ray beam is columnated and is larger than the largest crystallite, the spots from both the characteristic and continuous radiation will be approximately the same size and shape as the reflecting planes. If the specimen is not composed of randomly oriented crystallites then the spots will show a lack of randomness and the characteristic

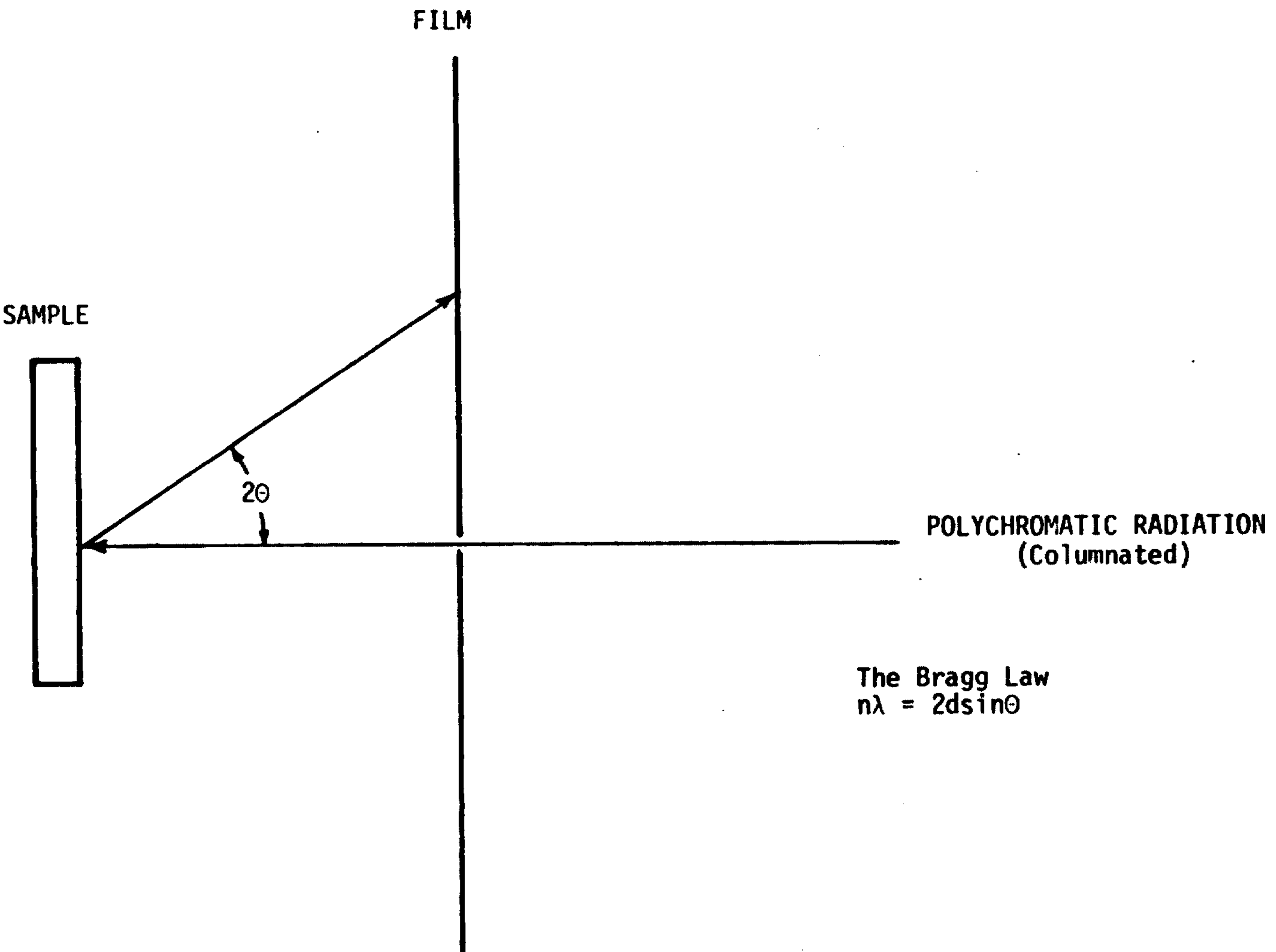

Figure B-1. Laue Camera Experimental Set-up for Investigating Possible Orientation in the CMS-4 Coatings

radiation rings will not be equally populated in all circumferential locations.

Three samples from CMS-4A were studied using this method. Spot sizes, and thus crystallite sizes, (beam divergence and camera geometry accounted for) were detected from $\approx$ 0.1 mm to 0.6 mm in diameter. Some of these showed shape features. These sizes cannot be viewed as inclusive because only those planes meeting the Bragg condition were seen and this is only a fraction of the total. Also, sizes smaller than 0.1 mm were not detectable by this procedure.

The samples were run at various positions on the surface and at various orientations with respect to the incident beam in an effort to find a positive indication of preferred orientation of the coatings. The results indicate that the orientation, if present, is very slight and not of the degree necessary to explain the large deviations in peak intensities. In one sample it was found that the larger crystallites did have some (probably small) degree of orientation since they seemed to be more densely populated on one portion of the characteristic cirular ring than at others. This was true over the face of the coating. However, the direction at which the more densely populated portion existed varied as the incident beam was moved to different spots on the surface.

All of this indicates that, although preferred orientation can still not be ruled out, there has been no indication of a strong degree of orientation. The crystallite sizes did vary considerably and the larger crystallites could be locally oriented but no long range orientation was detected for them either. The strong reflections from these large crystallites could significantly perturb the relative intensity

values obtained from the diffractometer with it's relatively small beam size. The relative intensity variations are therefore attributed to the broad range of crystallite sizes present in the sample. The possibility of a change in structure factor was not investigated since the only method available was to grind the coating off and x-ray it as a powder.

REFERENCES

1. Washburn, Malcolm E., Ceramic Bulletin, Vol. 46, No. 7, pp 667-671, (1967)

2. "A Computed X-Ray Diffraction Pattern for Alpha and Beta Silicon Nitride"; Gazsara, Charles P. and Reed, David; Army Materials and Mechanics Research Center, AMMRC TN 75-4, April (1975).

3. Dr. James E. Thomas, Pittsburg State University, Pittsburg, KS, Personal Communication

APPENDIX C

PROCESS SPECIFICATIONS

	Specification	Page
C.1	POWDER PREPARATION	C-1
C.2	HOT PRESSED CERAMIC SUBSTRATE FABRICATION	C-2
C.3	DIE SHAPE GRINDING	C-5
C.4	CNTD COATING APPLICATION	C-7

APPENDIX C

C.1 POWDER PREPARATION PROCESS SPECIFICATION

C.1.1 General - The ceramic bodies developed in this program were to be coated with pure CNTD ceramic coatings and therefore were not processed for maximum retention of purity.

C.1.2 Batch Size - 450 to 900 g of main constituent powders (SiC or Si_3N_4) plus appropriate weight percent of densification aid (B, MgO or Y_2O_3) and approximately 0.02 wt% Alcojet laboratory detergent as a surfactant.

C.1.3 Procedure

a) Mix dry powders in Al_2O_3 mortar and pestle.

b) Transfer powder to another container and add deionized H_2O or hexane (latter preferred if low oxygen content of powder is to be maintained) to the Al_2O_3 mortar in the ratio of approximately 375 cc liquid to 500 g powder.

c) Sift powder back into mortar and stir with pestle to avoid formation of lumps.

d) Transfer mix to Waring high speed laboratory blender with quart mixing jar and blend 15 minutes. Dry powder or liquid may need to be added in order to reach proper consistency which is that of a thick, peaky cake batter. Alternate method is to place powder and liquid in a one quart to one half gallon steel mill with steel balls ($\sim$ 1/2 total mill volume charge of balls) and mill 8 hrs.

e) Pour mix out into stainless steel trays and heat to 60 to 80°C overnight then vacuum dry at less than one mm Hg pressure for one hour, raising the temperature above 100°C.

f) Delump dried cake in Al_2O_3 mortar and pestle. Place broken cake (~ 100 g per charge) in a Spex Shatterbox and mill 5 minutes per charge.

g) Screen to -50 mesh and recycle +50 mesh to Shatterbox. Store -50 mesh material in polyethylene jars.

C.2 HOT PRESSED CERAMIC SUBSTRATE FABRICATION SPECIFICATION

C.2..1 Hot pressing will be performed in tooling of medium to high quality, fine grained graphite (ie. Great Lakes HLM-85, Union Carbide ATJ, Stackpole 2020, etc.).

C.2.2 All graphite surfaces to come in contact with the powder will be coated with two coatings of Aquadag (Acheson Colloids Company).

C.2.3 The properly prepared powder (Process Specification C.1) is loaded into the graphite tooling taking care to obtain a proper distribution of the powder. It is advisable to tamp the powder somewhat at the corners and edges of a rectangular cavity to offset a tendency for lower fabricated densities in those regions of the finished part.

C.2.4 The loaded tooling is cold pressed at a pressure equal to approximately 20% of the final hot pressing load, and placed in a vacuum preheater and elevated to approximately 300°C at a pressure < 1 mm Hg.

C.2.5 The loaded, cold pressed, outgassed tooling set is placed in the resistance heated, semicontinuous, horizontal hot press and pressed under flowing argon atmosphere. Optical temperature measurements are made at 5 minute intervals. The generalized hot press cycle is shown in Figure C-1 and the parameters for ceramic hardware fabrication are given in Table C-I. The run ending time, t_3, may vary slightly. The run is terminated when deformation rate during pressing falls below 0.001"/min.

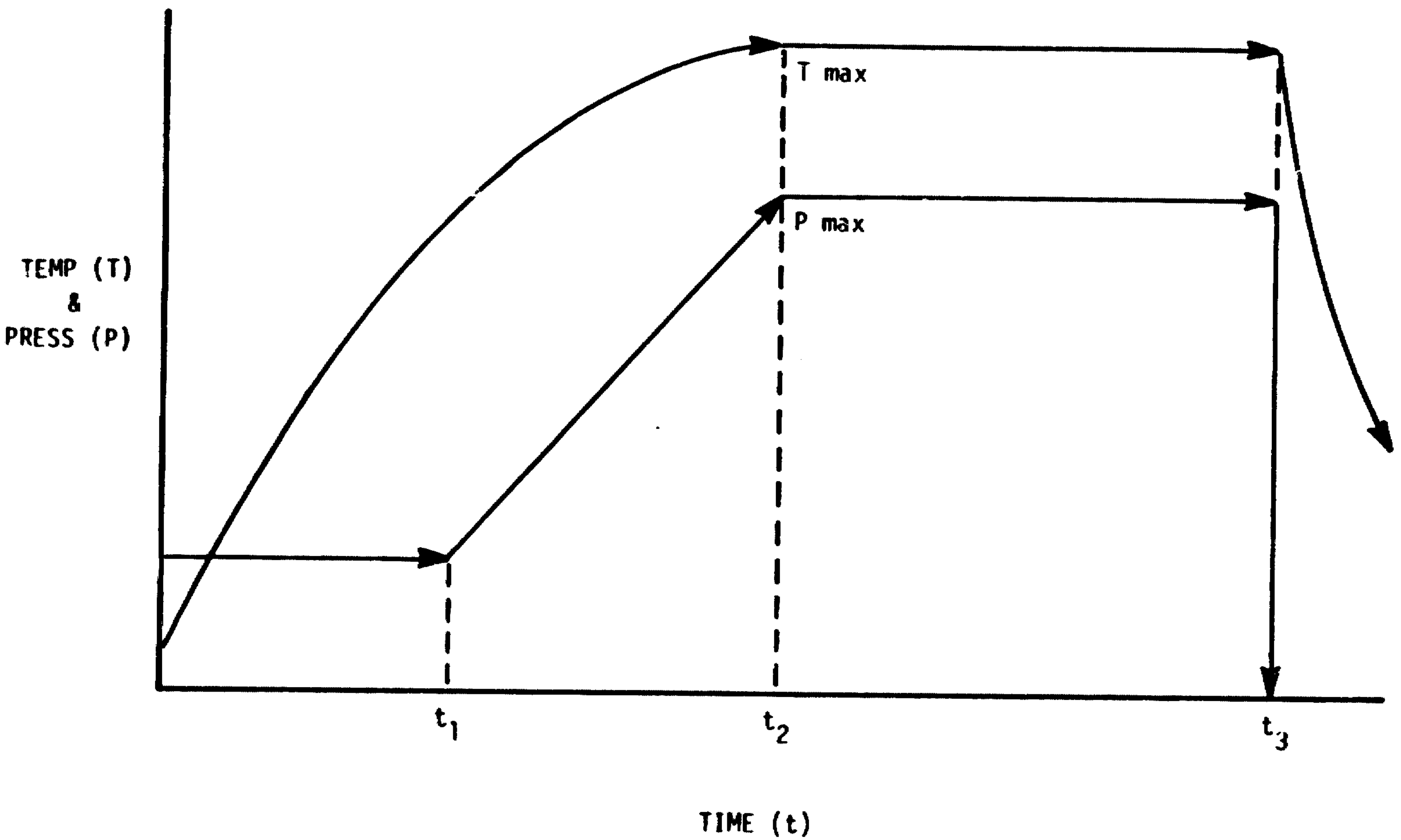

Figure C-1. Generalized Hot Pressing Cycle

Normally t_1 = 5 min., t_2 = 15 to 20 min.

TABLE C-I

PARAMETERS[1] FOR HOT PRESSING OF CERAMIC SUBSTRATES

Item Designation	t_3 (min)	T_{max} (^oC)	P_{max} (lb/in^2)
SiC (w/1 wt% B)			
Die Blanks	70	2300	3750
Containers	70	2320	2450
Si_3N_4 (w/4 wt% MgO)			
Die Blanks	35	1785	4375
Containers	80	1785	2450

[1] See Figure C-1

C.2.6 The pressed tooling is cooled; the part is removed and cleaned by sand blasting and the density is determined by bulk measurement or by immersion.

C.3 DIE SHAPE GRINDING PROCESS SPECIFICATION

C.3.1 The methods detailed in this specification are applicable for grinding either half of the Eagle-Picher Modified Two-Piece Die (Figure C-2), however only one half, Part A, will be addressed. This drawing, with appropriate surface identification added, is included on the following page.

C.3.2 The hot pressed die blanks should be approximately 0.150" thick, and should be ground to 0.123" thickness with two parallel faces (1 & 2).

C.3.3 The perimeter of the die shape is next established by sawing the blank to 1.2" X 1.05", maintaining perpendicularity of all corners by mounting surface 1 on a block using Aremco wafer-mount 562 hot mount material. The mounted blank is held in an indexable, rotatable (in the horizontal plane), x/y adjustable precision vise under the head of a horizontal surface grinder equipped with a diamond saw blade. This arrangement allows all the necessary cutting to be performed.

C.3.4 Without demounting the die blank the saw blade is exchanged for a grinding wheel approximately 0.25" wide and surface 3 is produced from surface 2 by removing 0.015" of material. The rotating capability of the vise is used to do the portion of surface 3 between the ends of the "runners" and the top of the die.

C.3.5 The blank is then demounted, flipped over, and remounted in a fixture having grooves to accept the "runners" of the die.

C.3.6 The mounted blank is fixtured on the angle for grinding surface 4, stopping when the correct "A" dimension is reached at the tip.

EAGLE-PICHER INDUSTRIES, INC.		
SPECIALTY MATERIALS DIVISION		
TWO PIECE DIE PART A, REV 1		
SCALE 4" = 1"		DATE 5 JANUARY 1979
DRAWN JMF	CHECKED	APPROVED
SHEET 1 of 2	DRAWING NO.	...CS-62, REV 1

NOTES:
1. UNLESS OTHERWISE NOTED ALL DIMENSIONS ARE IN INCHES
2. TOLERANCES UNLESS OTHERWISE NOTED:
   2 PLCS. = 0.01
   3 PLCS. = 0.003

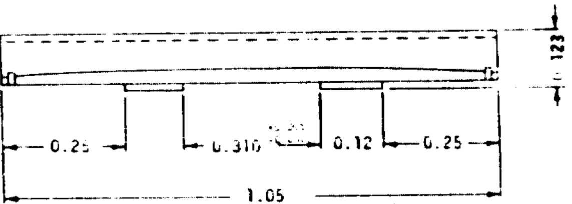

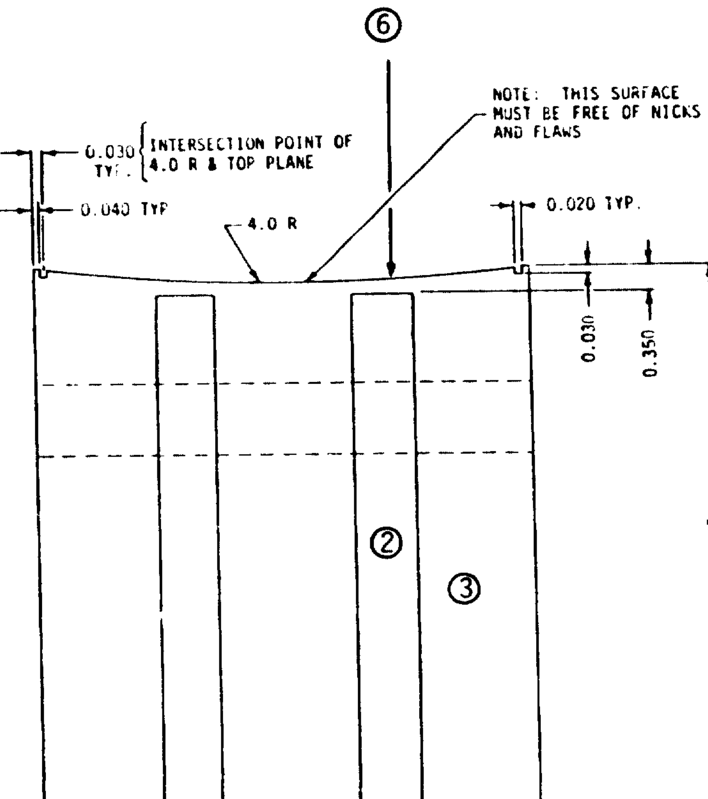

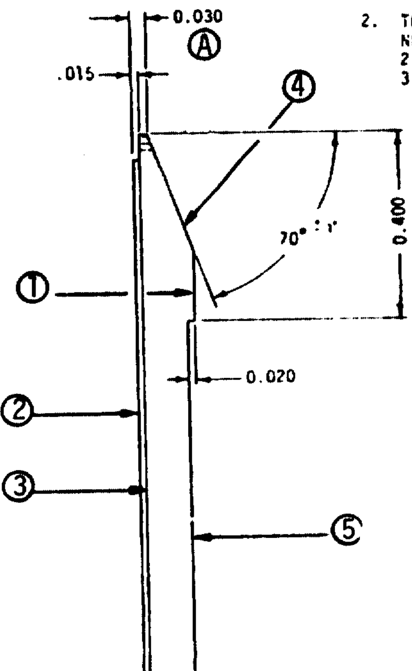

Figure C-2. Eagle-Picher Modified Two Piece Die Design, Part A

C.3.7 The mounted blank is held flat to the surface grinder chuck and surface 5 is produced.

C.3.8 The mounted blank is fixtured with the "top" up and surface 6 is ground with a 4.0" radius diamond wheel.

C.3.9 The final step is the addition of the saw cuts at the edges of the die top, and may be accomplished on the surface grinder or on a separate saw, using a blade 0.017" to 0.018" in width.

C.4 CNTD COATING APPLICATION PROCESS SPECIFICATIONS

Due to the proprietary and prexisting nature of the Chemetal CNTD fabrication process the process specification must remain confidential. Reference to the process specifications may be made as follows:

SiC Reference	1-4304-021 1-4406-139-146-021
Si_3N_4 Reference	1-4305-021 1-4306-254-280-021 16-4382-12-28-038
AlN Reference	1-4323-12-42-098
Si_2ON_2 Reference	1-4323-11-098
SiAlON Reference	1-4323-50-53-71-098

These deposition process specifications have been segregated and will be maintained without change for reference availability in future procurements.